

THREE DIMENSIONAL WAKE SURVEY BEHIND A
SHIP MODEL USING HOT-FILM ANEMOMETERS

CENTRE FOR NEWFOUNDLAND STUDIES

**TOTAL OF 10 PAGES ONLY
MAY BE XEROXED**

(Without Author's Permission)

KRISHNAN RAMANATHAN



Three Dimensional Wake Survey Behind a Ship Model
Using
Hot-Film Anemometers

by

Krishnan Ramanathan, B.Eng.

A Thesis Submitted to the School of Graduate Studies in Partial Fulfillment of the
Requirements for the Degree of Master of Engineering

Faculty of Engineering and Applied Science
Memorial University of Newfoundland
St. John's, Newfoundland

October 1995

St. John's

Newfoundland

Canada



National Library
of Canada

Acquisitions and
Bibliographic Services Branch

395 Wellington Street
Ottawa, Ontario
K1A 0N4

Bibliothèque nationale
du Canada

Direction des acquisitions et
des services bibliographiques

395, rue Wellington
Ottawa (Ontario)
K1A 0N4

Your file *Votre référence*

Our file *Notre référence*

The author has granted an irrevocable non-exclusive licence allowing the National Library of Canada to reproduce, loan, distribute or sell copies of his/her thesis by any means and in any form or format, making this thesis available to interested persons.

L'auteur a accordé une licence irrévocable et non exclusive permettant à la Bibliothèque nationale du Canada de reproduire, prêter, distribuer ou vendre des copies de sa thèse de quelque manière et sous quelque forme que ce soit pour mettre des exemplaires de cette thèse à la disposition des personnes intéressées.

The author retains ownership of the copyright in his/her thesis. Neither the thesis nor substantial extracts from it may be printed or otherwise reproduced without his/her permission.

L'auteur conserve la propriété du droit d'auteur qui protège sa thèse. Ni la thèse ni des extraits substantiels de celle-ci ne doivent être imprimés ou autrement reproduits sans son autorisation.

ISBN 0-612-13941-7

Canada

Abstract

This thesis presents results of investigative experiments using constant temperature anemometry to measure three dimensional flows in a towing tank.

A three dimensional probe was configured from three single 45° hot-film probes mounted with their sensor plane at 120° to each other. Presented are the calibration data for each of the single sensors for variations in velocity, yaw and pitch angles as well as the performance of the three probes when mounted in close proximity to each other. The calibration data of each sensor was fitted by a two parameter non-linear polynomial in velocity and yaw angle. The probes were insensitive to variations in angle of pitch.

A nominal wake survey was done with the three dimensional probe on the Institute of Marine Dynamics ship model No. M445, the model of a modern fishing vessel form. The results from this wake survey are compared with the results from an existing pitot tube wake survey done for this model. The spectrum of turbulence in the wake is presented.

Acknowledgements

First and foremost, I thank my supervisor, Dr. Neil Bose, Professor, Faculty of Engineering and Applied Science, for his unceasing encouragement and technical guidance throughout the course of this research work. I cannot adequately express my appreciation for his support.

I thank Dr. Shukai Wu, Research Officer, IMD, for assistance with probe calibrations and Mr. Carl Harris, Research Officer, for assistance with the model and pitot tube wake survey data. Thanks are due to Mr. Andrew Kuczora, Tank Technician, for his help during the experimental work.

I thank the School of Graduate Studies and the Faculty of Engineering and Applied Science for their financial support throughout the course of my study. In addition, I thank the Institute for Marine Dynamics for their partial financial support and for letting me use their wake rake and calibration rig. Last but not the least, I also thank my fellow colleagues for their helpful advice and constructive criticism.

Contents

Abstract	I
Acknowledgements	II
Contents	III
List of Figures	V
List of Tables	VII
Nomenclature	VIII
1. Introduction	1
1.1 Objectives of Study	3
2. Velocimetry Techniques	5
2.1 Pitot Tubes	5
2.2 LDV	6
2.3 CTA	9
3. Sensor Calibration	12
3.1 Calibration Procedure	12
3.2 Calibration Models	16
3.3 Calibration Results	19

4.	Wake Survey using CTA	47
4.1	Experimental Procedure	48
4.2	Wake Survey Results	50
4.3	Comparison of Results	64
4.4	Level and Frequency of Turbulence	68
5.	Discussion and Conclusions	73
	References	
	Bibliography	
	Appendix	

List of Figures

1.	Calibration setup	13
2.	Modified calibration rig	14
3.	Holder for 3-D configuration of probes	18
4.	Effect of varied overheat ratio (S5)	21
5.	Repeatability of normal calibration (S1)	23
6.	Repeatability of normal calibration (S2)	25
7.	Repeatability of normal calibration (S3)	27
8.	Repeatability of normal calibration (S5)	29
9.	Effect of varied pitch angle (S1)	31
10.	Effect of varied pitch angle (S2)	33
11.	Effect of varied pitch angle (S3)	35
12.	Effect of varied pitch angle (S3)	37
13.	Effect of varied pitch angle (S5)	39
14.	Yaw-pitch calibration (S3)	41
15.	Yaw calibration (S1)	43
16.	Yaw calibration (S2)	44
17.	Yaw calibration (S3)	45
18.	Yaw calibration (S5)	46

List of Tables

1.	Normal calibration with varied overheat ratio	22
2.	Normal calibration (S1)	24
3.	Normal calibration (S2)	26
4.	Normal calibration (S3)	28
5.	Normal calibration (S5)	30
6.	Pitch calibration (S1)	32
7.	Pitch calibration (S2)	34
8.	Pitch calibration (S3)	36
9.	Pitch calibration (S3)	38
10.	Pitch calibration (S5)	40
11.	Yaw-pitch calibration (S3)	42
12.	Model particulars	49
13.	Pitot tube wake survey data (radius - 5.08 cm)	56
14.	Pitot tube wake survey data (radius - 6.98 cm)	57
15.	Pitot tube wake survey data (radius - 8.89 cm)	58
16.	Pitot tube wake survey data (radius - 10.67 cm)	59
17.	Pitot tube wake survey data (radius - 12.19 cm)	60

Nomenclature

- CTA - Constant temperature anemometer
- IMD - Institute for Marine Dynamics
- MUN - Memorial University of Newfoundland
- U_x - Normal speed in x direction
- U_y - Normal speed in y direction
- U_z - Normal speed in z direction
- α_1 - Yaw angle for sensor 1
- α_2 - Yaw angle for sensor 2
- α_3 - Yaw angle for sensor 3
- α_5 - Yaw angle for sensor 5
- S1 - Sensor 1
- S2 - Sensor 2
- S3 - Sensor 3
- S5 - Sensor 5
- m - Order of polynomial
- a - Overheat ratio
- n - Exponent, an experimental constant
- k - Index of terms of a polynomial, $k = 0,1,2,3,\dots,m$

V_c - Curve fitted voltage

CW - Clockwise

ACW - Anticlockwise

U_{ass} - Assumed velocity in test data analysis

U_{cal} - Calculated velocity in test data analysis

CHAPTER ONE

Introduction

Constant temperature anemometry was first employed by L.V. King in the early part of this century [Perry (1982)]. Though advances have been made over the years, use of the instrument has predominantly been for measurements in air. Application of constant temperature anemometry for measurements in water, which requires use of hot-film sensors with thick quartz coatings, has received less attention. Most of the published experiments in water were done in water channels under controlled conditions. Measurements in other fluid medium such as polymer solutions, mercury, blood, glycerine and oil are possible with special probes designed for such specific applications [Lomas (1986)].

The most commonly reported problems encountered with use of hot-film sensors in water include sensor contamination, air bubbles on the sensor at high overheat ratio, thermal instability during the burn in period and uncontrolled environment (varying temperatures). Calibration of sensors at high overheat ratios results in bubble formation which is detrimental to the sensors and affect their response [Wu and Bose (1992)]. Sufficient time has to be allowed for sensors to become stable before any measurements

can be done [Wu and Bose (1991)]. In addition, sensors are sensitive to changes in water temperature in the towing tank. Variation of fluid temperature during the calibration and testing process has a more pronounced effect in water than in air; the reason being that low overheating ratios are used in water to prevent bubble formation and boiling. A change of 2°C in water temperature causes an error of 26% in measured velocity [Resch (1969)]. In such uncontrolled conditions, normal calibrations have to be repeated before any test is carried out. Alternatively, by closely monitoring the water temperature and applying an appropriate correction to the calibration, temperature variations can be accounted for. Various methods for temperature correction have been suggested by researchers in the past. Temperature compensation can be obtained by evaluating the fluid properties at the mean film temperature [Rahman et al. (1987)]. The concept of varying overheat resistance provides results which represent hot-wire output response to variations in fluid temperature [Hollasch and Gebhart (1971)].

Sensor contamination leads to a drift in the anemometer output voltage. However, the contamination does not affect the frequency response of the probes up to 200 Hz, since for this range the penetration depth of thermal fluctuations is much larger than the thickness of any dirt layer [Jimenez et al. (1981)]. Tests at constant velocity showed that, for cylindrical sensors, drift was a function of dirt particle size to sensor radius [Morrow and Kline (1974)]. A conical-type probe has been used in water flows because its contamination by dirt particles is less than that for other design [Okuno (1988)].

Successful calibration of the quartz-coated sensors in water has led to the use of two sensors (X-configuration and vee sensors) and triple sensors for studying turbulent flow [Johnson and Eckelmann (1984)]. The effects of mechanical interference between sensors, as in the case of X-probes, could be severe, depending on the size of the probes [Fernando et al. (1988)]. A multi-sensor hot wire probe can be used to measure vorticity and velocity in turbulent flows [Vukoslavcencic et al. (1989)].

Directional sensitivity, alignment of the sensor perpendicular to the axial velocity component, is a key issue in the calibration of hot film probes. Errors in calibration, velocity and turbulence measurement using a hot wire/film probe depend on the directional sensitivity of the probe [Okuno (1988)]. Measures have been taken by researchers to overcome the forward-reverse ambiguity in highly turbulent flows. Hot wire probes have been used to obtain the three components of mean velocities and six components of Reynolds' stresses [Lakshminarayana et al. (1982)]. However, such work has so far been limited mainly to measurements in air.

1.1 Objectives of Study

The aim of this work was to investigate the use of constant temperature anemometry to measure three dimensional flows in a towing tank. The work included the following parts.

- * Calibrate hot-film sensors using constant temperature anemometers and investigate

the effect of changes in velocity, yaw and pitch angles on sensor output.

- * Investigate the effectiveness of use of three 45° hot film sensors to measure 3-D flow fields.
- * Conduct a nominal wake test on a round bilge fishing vessel model.
- * Compare the results with data previously obtained from a pitot tube wake survey done on the same model, at a speed of 0.54 m/s.
- * Study the turbulence spectrum in the wake of the ship model.

CHAPTER TWO

Velocimetry Techniques

This chapter presents an overview of the various methods used to determine the magnitude and direction of fluid velocity. Emphasis is put on those techniques which have found application in hydrodynamic testing facilities such as towing tanks and cavitation tunnels. The use of constant temperature anemometry, being the prime objective of this work, has been discussed in detail.

2.1 Pitot Tubes

In spite of the development of constant temperature anemometry and laser doppler velocimetry, pitot tubes are still used extensively for fluid flow measurements. A conventional pitot tube in conjunction with water tube manometers can be used for pressure measurements which are later translated into velocity. The development of electronic pressure transducers and the reduction in the size of the pitot tube, which otherwise affect the true flow pattern, have helped researchers to reduce some of the errors in measurements.

Pitot tubes, apart from being relatively cheap, are mechanically simple and extremely robust for such applications. With appropriate pressure sensors, they can be used over a wide range of flow velocities. A major disadvantage of pitot tubes is that, their presence in the flow tends to disturb/misread the actual flow pattern. In turbulent flows, pitot tube results are prone to errors, for the reason that only a single mean velocity is obtained. The water column dynamics in the manometers does not permit turbulence measurement. Calibration of the system is done in two phases; one being the transducer output voltage against pressure, and the other being probe tip geometry against inflow angle. The probe tip geometry influences the range of inflow angle that can be measured. The practical upper limit on inflow angles for both spherical and conical tip pitot tubes is about 35° [Harris (1993)].

2.2 Laser Doppler Velocimetry

Laser doppler velocimetry is the most commonly encountered non-intrusive technique used for fluid flow measurements. By analogy with hot-wire anemometers, laser velocimeters used for the determination of fluid velocities are referred to as laser anemometers.

A laser doppler velocimeter measures velocity by measuring the doppler shift in the frequency of laser light from incident and reflected light from microscopic particles within the flow. Laser doppler velocimeters, like constant temperature anemometers,

provide information on the turbulent nature of the flow which cannot be obtained with pitot tubes or other mechanical devices.

A laser doppler velocimeter has high spatial and temporal resolution depending on the quality and quantity of the scattered particles. The density of seeding particle concentration is a critical factor for LDA operation and effectively determines the data sampling rate. In some instances, the dirt particles inherent in the flow are sufficient, while in other cases artificial seed particles are introduced in the flow. These dirt particles, also referred to as scattering centres, may vary in size from a fraction of a μm to several tens of μm for efficient operation. Particles which are too small will not produce enough scattered power to exceed the noise level of the detection system. Particles which are too large, on the other hand, will tend to block the light completely and thus render the instrument inoperative. In effect, sampling rates for laser doppler velocimeter and the accuracy of measurement depend on the optical arrangements, detector, particle statistics, fluid medium, test speed, anticipated levels of turbulence and finally on the approach to electronic signal processing [Durrani et. al. (1977)].

A major disadvantage of laser doppler velocimeter is that the measurement is not continuous, unlike that from constant temperature anemometers. It gives measurements at various instants of time. Also, measurements are not made directly of velocity. Instead, these instruments measure velocities of particles in fluids, i.e. seed or dirt particles, which may or may not follow at the fluid velocity. The discrepancy between

particle velocities in fluids and fluid velocities may be significant for large particles especially in turbulent flows [Durrani et. al. (1977)]. Only particles as small as $0.1 \mu\text{m}$ can faithfully follow turbulent flow in liquids such as water [Watasiewicz et. al. (1976)].

Laser doppler velocimetry has three fundamental advantages over constant temperature anemometry. Firstly, there is no flow interference since the probe is purely optical. Secondly, the system does not require calibration as fluid velocity is measured directly from the doppler shift in the frequency of coherent light reflected from scattering centres. Thirdly, the instrument measures the component of velocity in a specified direction, the output being a linear function of this velocity component.

In principle, laser doppler velocimeter measurements are non-intrusive in nature except for the addition of seed particles to increase data acquisition rates to an acceptable level. However, implementation of a laser doppler velocimeter system may become very intrusive depending on the test facility and arrangement of the optical system. For measurements in cavitation tunnels and small open water channels, the optical system can be external to the flow. For towing tank applications, this equipment has either to be placed directly in the flow or the laser beam has to be routed through an optical conduit immersed in the flow. In the latter case, the optical conduit will absorb some of the laser light energy making less available to the interrogation beams. A laser doppler velocimeter system costs as much as 10 times that of a constant temperature anemometer system and because of this their use has been restricted.

2.3 Constant Temperature Anemometry

Hot-film anemometry and hot-wire anemometry work on the same principle except that the geometry of the sensors is different. The hot-film anemometer is basically a thermal transducer. The principle of operation is as follows: an electric current is passed through a fine filament which is exposed to the flow. As the flow rate varies, the heat transfer from the filament varies. This in turn causes a variation in the heat balance of the filament. The filament is made from a material which possesses a temperature coefficient of resistance. The variation of resistance is monitored by various electronic methods which give signals related to the variations in flow velocity or flow temperature.

There are three modes of operation of a hot-film system. First is the constant temperature mode where the filament is placed in a feedback circuit which tends to maintain the film at constant resistance and hence constant temperature. The second is the constant current mode where the current in the wire is kept constant and variations in wire resistance caused by the flow are measured by monitoring the voltage drop across the filament. A third type, the pulsed wire anemometer, measures velocity by momentarily heating a film to heat the fluid around it. This spot of heated fluid is convected downstream to a second film that acts as a temperature sensor. The time of flight of the hot spot is inversely proportional to the fluid velocity. Of the three modes described above, the constant temperature mode is the most frequently used. The reason

for this is that the feedback mechanism/servo mechanism responds rapidly and the sensor temperature remains virtually constant. The voltage difference across the bridge is related to the fluid velocity.

Heat transfer/cooling rate can be attributed to all of the following.

1. Heat loss from a hot-film sensor by convection to the fluid.
2. Heat loss from a hot-film sensor by conduction to the support needles.
3. Heat loss from the hot-film sensor by radiation to cooler surroundings.
4. Storage of heat in the hot-film sensor.

King's law, by far the most well-known of the heat transfer laws used in hot-film anemometry, is written as,

$$V^2 = A + BU^n \quad (1)$$

where V is the anemometer output voltage taken across the Wheatstone bridge in the electronics package, U is the fluid velocity, n is an experimentally determined constant, and A & B are experimental constants. Various modelling techniques have been developed over the years which have been discussed in chapter 3.

Hot-wire anemometry was originally developed for use in gaseous flow fields but the delicacy of wire probes prohibited their use in harsh or conductive media. However, the development of film sensors heavily coated with quartz have been used successfully in fluid applications. The quartz coating protects the sensors from contaminants,

electrical and thermal damage. The dimensions of the sensors are of the order of microns which hardly affects the flow pattern.

A distinct advantage of hot-film anemometry is that the output from the sensor is continuous with an extremely low response time and this reveals information on the turbulence characteristics of the flow. It is possible to determine a mean flow component from the sensor output, but a measurement can also be obtained of the level and frequency of turbulence present in the flow. Sensors, once put through the burn-in period, can be calibrated for varied angles of pitch and yaw. It is pertinent to carry out the entire calibration process at the same overheat ratio.

For the following reasons, constant temperature anemometry has advantages over other techniques :

1. Hot film probes are less intrusive to the flow than most pitot tube assemblies.
2. High spatial resolution is accomplished.
3. The short response time permits investigations of high frequency flow fluctuations.
4. The high flow sensitivity permits detection and measurement of very low flow velocities.
5. Low cost compared to laser doppler velocimetry.
6. Continuous response to the flow characteristics.

Chapter Three

Sensor Calibration

Before a wake survey could be done successfully, it was necessary to determine the sensitivity of each sensor to flow velocity, magnitude and direction. By this means, the characteristics of each sensor was established. A direct relationship between the velocity and the measured output voltage, for each sensor, results in a calibration curve. Previous experience had shown that it was necessary to burn in the sensors adequately in order to ensure stable behaviour. A small channel was used for this purpose. During this phase, periodical normal calibrations were done in order to ensure a stable behaviour. It was found that a sensor took nearly 60-70 hours to stabilize. This phenomenon was also observed with wedge shaped sensors when used for flow measurements in water [Wu and Bose (1992)].

3.1 Calibration Procedure

Though there are numerous ways employed to calibrate sensors, calibration of individual sensors was done in a towing tank. Three constant temperature anemometers

type 55M10 (CTA) and five 45° hot film sensors type 55R12, manufactured by Dantec Electronics Inc., were available for this research work. Description of the CTAs, hot film sensors and the electronic circuitry associated with constant temperature anemometry have been detailed in the manual published by Dantec Electronics. Each 45° hot-film sensor was held individually at the end of a rod connected to the calibration rig. At the end of the rod was a hole drilled at 45°, to accommodate the sensor. This was done in order to calibrate each sensor in a direction normal to the sensor film. Scales attached to the rod allowed changes to be made in pitch and yaw angles. Perpendicularity of the rod was ensured by using a plumb line and by calibrating at slight changes in yaw angle on either side of the zero reading on the protractor. Figures 1 and 2 show the calibration arrangement.



Fig 1 : Calibration Setup

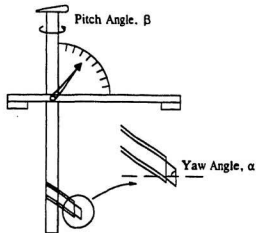


Fig. 2 : Modified Calibration Rig

The towing carriage was operated at known speeds and the voltage outputs from the sensors were recorded. Data of carriage speed and sensor output were recorded on a micro computer through a Keithley 575 16 bit A/D convertor. Two channels were used, one for carriage velocity and the other for sensor output voltage.

The sensors were set at an overheat ratio of 0.4 during the entire calibration process. The overheat ratio was calculated based on the temperature of the fluid medium (T_w) and the temperature of the sensor (T_s). Overheat ratio, a , can be expressed as

$$a = (T_s - T_w) / T_s \quad (2)$$

A constant decade resistance setting in the anemometer helped maintain a constant overheat ratio. Water temperature was recorded before commencement of calibration and the sensor temperature thereby obtained was used to set the decade resistance. The formula used to set the decade resistance is

$$R_d = R_t + [\alpha \times R_s (T_s - T_w)] \quad (3)$$

where R_d is the decade resistance, R_t is the total resistance of the sensor including the lead resistance, α is the temperature coefficient of resistivity and R_s is the sensor resistance.

Firstly, sensor 3 was calibrated for pitch and yaw angles. During the initial stages of calibration, it was found that this sensor was sensitive to pitch; which after several runs disappeared. It is possible that the sensor, though put through the burn in period, was not burnt in adequately on the sides. These hot film sensors have a very small rectangular cross section nickel film and are coated with a 2 μm layer of quartz. Following an adequate burn in period, the sensor was found to be insensitive to changes in pitch angle and yaw calibrations were done. As the sensor output depends on the rate of heat transfer, the effective area normal to the flow is reduced as the yaw angle is increased. Once the behaviour of the sensor was known, calibrations of sensor 2 and sensor 1 were done and these showed similar trends to sensor 3. During the burn in process, sensor 4 was accidentally burnt out. Three sensors were needed for the wake survey. Sensor 5 was calibrated as a spare. Normal, pitch and yaw calibrations for all four sensors were done in November and December of 1993.

3.2 Calibration Models

King's law is usually expressed as

$$V^2 = A + BU^n \quad (4)$$

where V is the anemometer output voltage, U is the fluid velocity flowing past the sensor, and A and B are experimental constants. King, based on his experiments, found the magnitude of the exponent n to be 0.5 [King (1914)].

A general form of modified King's law is written as

$$V^2 = \sum_{k=0}^m A_k U^{kn} \quad (5)$$

where V is the voltage, U is the velocity of the fluid, m is the order of the polynomial, A_k and exponent n are experimental constants [Wu and Bose (1992)]. This calibration model was used to analyze pitch and normal calibration data for all sensors.

In the case of a 3-D flow, the sensor is cooled by the velocity components in all directions, but its sensitivity to each component differs. The heat loss in this case depends on the effective cooling velocity, U_e , which should replace U in the above equation. For such cases, the effective cooling velocity is expressed as

$$U_e^2 = U_n^2 + k_i^2 U_i^2 + k_p^2 U_p^2 \quad (6)$$

where k_i and k_p are the yaw and pitch factors respectively [Champagne et al. (1967)]. This method assumes the yaw factor to be constant over the entire velocity range.

However, it has been found that the yaw factor showed strong velocity dependence at low velocities [Wu and Bose (1994)].

A two-variable non-linear polynomial of the form

$$V^2 = \sum_{i=0}^m \sum_{j=0}^k A_{ij} U^i \alpha^{kj} \quad (7)$$

was proposed as a better calibration model [Wu and Bose (1993)]. In the above equation, α is the yaw angle, m is the order of the polynomial and k is subscript of polynomial of m th order. Yaw calibration data for each sensor was fitted using a least squares fit program based on the above equation. Coefficients obtained, for a polynomial of order 3 ($m=3$), were used to analyze test data. Polynomial of order 2 gave an error which was larger than that obtained using a polynomial of 3rd order.

Water temperature changed significantly during the calibration process. Initially, the anemometer was set such that the sensors worked at an overheat ratio of 0.4. The decade resistance setting on the CTA was left untouched in spite of temperature fluctuations. Temperature was recorded during every calibration process. Effectively, the sensors were allowed to operate at slightly varying overheat ratios. In order to accurately determine the characteristics of the sensor for varied overheat ratio, a series of runs was made using sensor 5, operated at overheat ratios ranging from 0.2 to 0.4. Calibration voltage, in addition to curve-fitted voltage and percentage error at each point, is given in table 1. A plot of the normal calibrations at various overheat ratios shows that the voltage level from the sensor at a given speed increased with an increase in overheat ratios and

vice-versa (fig. 4).

For simultaneous calibration of the three sensors, oriented at 120° apart, a holder was made up which could also be used for the wake survey (fig. 3). It was decided not to disturb the orientation of the sensors after calibration; once mounted in the holder, the same sensor and holder assembly was used for both the calibration and tests. Sensors 1,3 and 5 were chosen for wake tests due to their steady performance during the calibration process. Adequate yaw calibration data was not available for sensor 2.

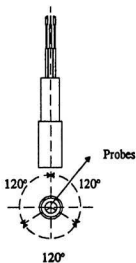


Fig. 3 : Holder for 3-D configuration of probes

3.3 Calibration Results

Normal calibrations were repeated on different days to check if the sensor responses were stable at a given overheat ratio. Modelling / curve-fitting of normal calibration data was based on the modified form of King's law (eqn. 5). A third order polynomial was chosen over a second order polynomial for the reason that a better curve fit with minimum curve fitting error was achieved.

Figures 5,6,7 and 8 are indicative of repeatability levels of normal calibration for sensors 1,2,3 and 5 respectively. Tables 2,3,4 and 5 contain corresponding calibration data points, curve-fitted voltage (V_c) and the percentage error (% Error) in curve fit at every point. The response of each sensor was almost the same for calibrations done either twice on the same day or over a span of 2 to 3 days.

Figures 9,10,12 and 13 are indicative of the insensitivity of the four sensors to variation in pitch angles. Tables 6,7,9 and 10 contain their corresponding calibration data and curve fitting error at each point. Also, the normal calibration for each sensor had good correspondence with the pitch calibration. Pitch calibration data were modelled based on a third order polynomial of the modified King's law (eqn. 5). Curve fitting errors were negligible and hence the modified form of King's law was adequate to check for repeatability of normal calibration. Though there were slight variations in sensor

response during pitch calibration, this was not as significant as in yaw calibrations. Hence, it was assumed that the sensors were insensitive to changes in pitch angle. Figure 11 indicates the levels of sensitivity of sensor 3 to changes in angles of pitch observed in the earlier stages of the burn in period; these reduced after further burn in. Table 8, corresponds to this initial pitch calibration plot.

Yaw calibration was modelled based on the two-variable non-linear polynomial of order 3 (eqn. 7), for the four sensors. The method of yaw factor modelling (eqn. 6) assumes that the yaw factor is constant for any given angle, over a range of velocity. As discussed earlier, this is not necessarily true at lower speeds. Figures 15,16,17 and 18 show the yaw characteristics of the sensors. Maximum heat transfer occurs when the sensor plane is at 90° to the flow direction, i.e. the normal projected area to the flow is maximum. Also, heat transfer is minimum when the sensor plane is parallel to the direction of flow, i.e. the normal projected area to the flow is minimum. The yaw calibration data, coefficients of the polynomials and the percentage error at each point can be found in the appendix, along with the computer program used for analysis. It can be seen that the curve-fitting error based on this model, at most points in the region of interest (0.54 m/s), was under 0.7 %.

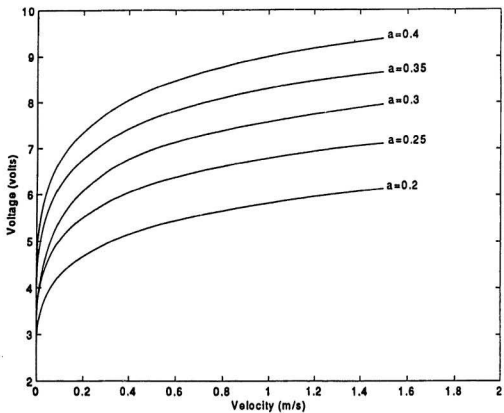


Fig. 4 : Effect of Varied Overheat Ratio (S5)

a = 0.20

Velocity	Voltage	Vc	% Error
0.0000	2.5261	2.5331	0.2744
0.1216	4.3993	4.3705	0.6518
0.2471	4.8147	4.8084	0.1304
0.4996	5.2363	5.3070	1.3494
0.7511	5.6072	5.6157	0.1513
1.0034	5.9135	5.8370	1.2939
1.2554	6.0040	6.0049	0.0155
1.5064	6.1099	6.1364	0.4338

a = 0.25

Velocity	Voltage	Vc	% Error
0.0000	2.9036	2.9059	0.0801
0.1216	5.1570	5.1511	0.1146
0.2479	5.6849	5.6637	0.3729
0.4988	6.1465	6.2266	1.3037
0.7506	6.6277	6.5676	0.9062
1.0030	6.8344	6.8041	0.4436
1.2546	6.9268	6.9769	0.7227
1.5062	7.1206	7.1070	0.1910

a = 0.30

Velocity	Voltage	Vc	% Error
0.0000	3.1735	3.1767	0.0955
0.1213	5.6448	5.6093	0.6219
0.2471	6.2147	6.2854	1.1365
0.4994	7.0239	6.9666	0.8187
0.7510	7.3504	7.3373	0.1785
1.0029	7.5103	7.5876	1.0312
1.2542	7.8413	7.7837	0.7334
1.5060	7.9447	7.9586	0.1737

a = 0.35

Velocity	Voltage	Vc	% Error
0.0000	3.5427	3.5487	0.1679
0.1224	6.3709	6.3442	0.4179
0.2478	6.9622	6.9589	0.0466
0.4994	7.5588	7.6342	0.9974
0.7514	8.0679	8.0367	0.3876
1.0027	8.3437	8.3107	0.3965
1.2546	8.5166	8.5089	0.0907
1.5056	8.6327	8.6548	0.2561

a = 0.40

Velocity	Voltage	Vc	% Error
0.0000	3.8870	3.8897	0.0689
0.1212	6.9107	6.8920	0.2709
0.2481	7.5363	7.5525	0.2147
0.4998	8.2568	8.2697	0.1567
0.7512	8.7035	8.7003	0.0371
1.0046	9.0154	9.0002	0.1685
1.2561	9.2221	9.2187	0.0369
1.5071	9.3745	9.3837	0.0979

Table 1 : Normal Calibration with Varied Overheat Ratio(S5)

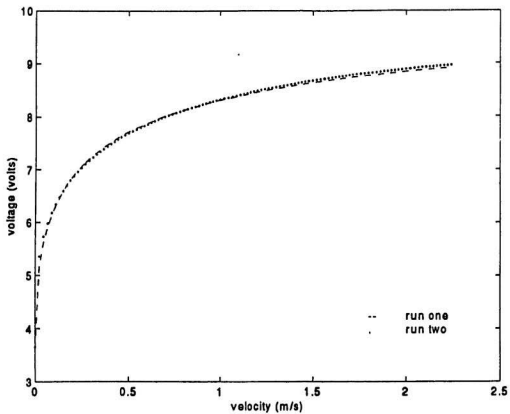


Fig. 5 : Repeatability of Normal Calibration (S1)

Run # 1

Velocity	Voltage	Vc	% Error
0.0000	3.6193	3.6192	0.0016
0.1220	6.4724	6.4762	0.0583
0.2471	7.0906	7.0825	0.1141
0.4993	7.7061	7.7092	0.0404
0.7502	8.0618	8.0685	0.0834
1.1044	8.3991	8.3963	0.0332
1.4556	8.6293	8.6158	0.1566
1.8072	8.7601	8.7754	0.1744
2.2607	8.9298	8.9254	0.0491

Run # 2

Velocity	Voltage	Vc	% Error
0.0000	3.6475	3.6478	0.0069
0.1217	6.4822	6.4817	0.0069
0.2468	7.0544	7.0544	0.0005
0.4991	7.6886	7.6844	0.0549
0.7508	8.0542	8.0631	0.1100
1.2545	8.5312	8.5262	0.0588
1.7576	8.8009	8.8002	0.0076
2.2613	8.9724	8.9737	0.0148

Table 2 : Normal Calibration (S1)

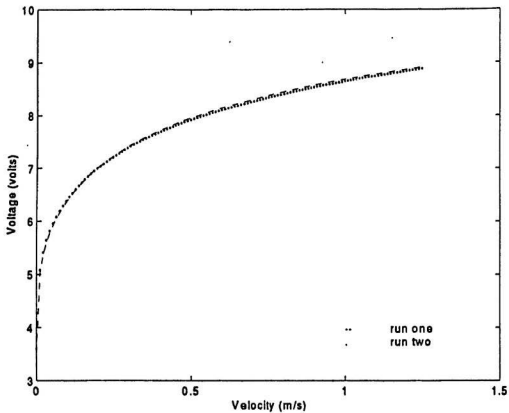


Fig. 6 : Repeatability of Normal Calibration (S2)

Run # 1

Velocity	Voltage	Vc	% Error
0.0000	3.5292	3.5309	0.0473
0.1218	6.6103	6.5958	0.2188
0.2473	7.2211	7.2363	0.2105
0.4998	7.9349	7.9459	0.1393
0.7506	8.3892	8.3746	0.1758
1.0045	8.6864	8.6800	0.0730
1.2554	8.8539	8.9068	0.0892

Run # 2

Velocity	Voltage	Vc	% Error
0.0000	3.5973	3.5997	0.0649
0.1214	6.6239	6.6054	0.2821
0.2473	7.2078	7.2243	0.2304
0.4999	7.9049	7.9136	0.1104
0.7512	8.3154	8.3377	0.2688
1.0034	8.7065	8.6435	0.7228
1.2547	8.8458	8.8781	0.3651

Table 3 : Normal Calibration (S2)

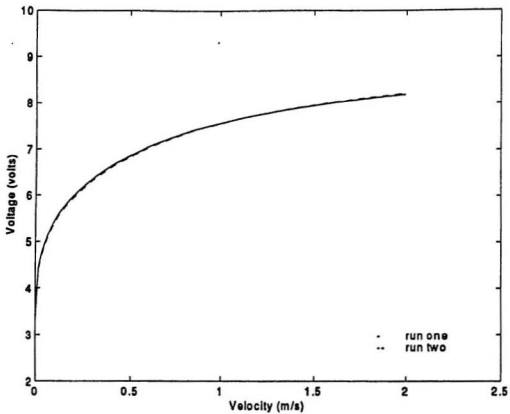


Fig. 7 : Repeatability of Normal Calibration (S3)

Run # 1

Velocity	Voltage	Vc	% Error
0.0000	3.3487	3.3588	0.2983
0.1213	5.6040	5.5504	0.9559
0.2478	6.1085	6.1444	0.5882
0.4992	6.7717	6.8242	0.7757
0.7511	7.2852	7.2511	0.4676
1.0033	7.5658	7.5552	0.1407
1.2546	7.7999	7.7823	0.2198
1.5066	7.9481	7.9588	0.1341
1.7581	8.0850	8.0956	0.1308
2.0090	8.2043	8.2017	0.0307

Run # 2

Velocity	Voltage	Vc	% Error
0.0000	3.3556	3.3635	0.2341
0.1212	5.6406	5.5884	0.9256
0.2474	6.1217	6.1759	0.8851
0.4908	6.8338	6.8479	0.2061
0.7524	7.2853	7.2659	0.2670
1.0020	7.5620	7.5585	0.0464
1.2536	7.7894	7.7794	0.1287
1.5063	7.9424	7.9496	0.0899
1.7549	8.0775	8.0794	0.0232
2.0096	8.1808	8.1822	0.0172

Table 4 : Normal Calibration (S3)

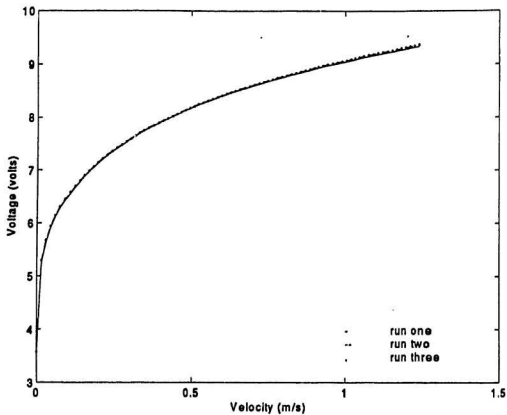


Fig. 8 : Repeatability of Normal Calibration (S5)

Run # 1

Velocity	Voltage	Vc	% Error
0.0000	3.6314	3.6339	0.0685
0.1215	6.7202	6.6995	0.3123
0.2478	7.3662	7.3848	0.2511
0.4995	8.1504	8.1731	0.2774
0.7509	8.6999	8.6820	0.1925
1.0028	9.0872	9.0630	0.2665
1.2546	9.3486	9.3674	0.2013

Run # 2

Velocity	Voltage	Vc	% Error
0.0000	3.5486	3.5514	0.0788
0.1222	6.7131	6.6908	0.3317
0.2476	7.3560	7.3745	0.2518
0.4988	8.1376	8.1617	0.2950
0.7504	8.6796	8.6677	0.1363
1.0029	9.0783	9.0445	0.3721
1.2550	9.3201	9.3432	0.2483

Run # 3

Velocity	Voltage	Vc	% Error
0.0000	3.5687	3.5706	0.0538
0.1223	6.7266	6.7099	0.2446
0.2473	7.3691	7.3818	0.1725
0.4998	8.1498	8.1698	0.2456
0.7515	8.6866	8.6812	0.0620
1.0018	9.0987	9.0649	0.3729
1.2550	9.3566	9.3782	0.2300

Table 5 : Normal Calibration (S5)

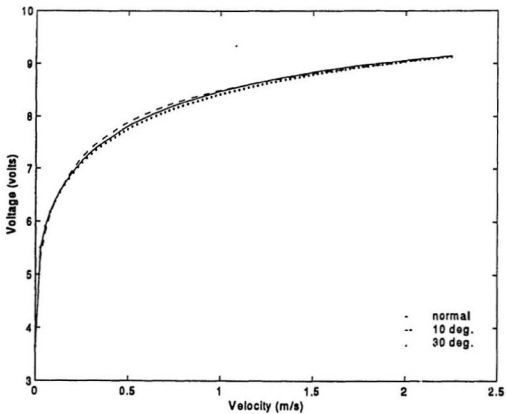


Fig. 9 : Effect of Varied Pitch Angle (S1)

Normal

Velocity	Voltage	Vc	% Error
0.0000	3.5939	3.5961	0.0601
0.1219	6.5749	6.5424	0.4947
0.2475	7.0887	7.1401	0.7253
0.5001	7.8063	7.7971	0.1168
0.7516	8.2098	8.1923	0.2136
1.2551	8.6819	8.6773	0.0533
1.7595	8.9479	8.9668	0.2111
2.2620	9.1592	9.1511	0.0885

10 degrees

Velocity	Voltage	Vc	% Error
0.0000	3.6295	3.6284	0.0428
0.1217	6.5282	6.5434	0.2461
0.2480	7.2349	7.2069	0.3888
0.5003	7.8602	7.8733	0.1602
0.7510	8.2301	8.2408	0.1252
1.2549	8.6864	8.6689	0.1979
1.7569	8.9252	8.9346	0.1105
2.2622	9.1462	9.1444	0.0229

30 degrees

Velocity	Voltage	Vc	% Error
0.0000	3.6399	3.6445	0.1260
0.1208	6.5306	6.5183	0.1868
0.2477	7.1232	7.1058	0.2438
0.5004	7.7222	7.7478	0.3310
0.7518	8.0960	8.1386	0.5254
1.2539	8.6871	8.6281	0.6801
1.7575	8.9262	8.9322	0.0667
2.2612	9.1257	9.1368	0.1221

Table 6 : Pitch Calibration (S1)

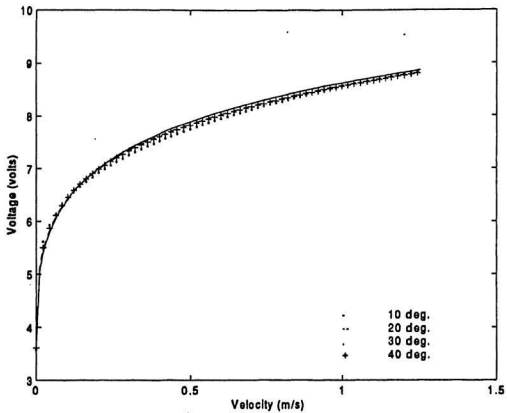


Fig. 10 : Effect of Varied Pitch Angle (S2)

10 degrees

Velocity	Voltage	Vc	% Error
0.0000	3.5947	3.5963	0.0428
0.1222	6.5970	6.5808	0.2408
0.2477	7.1713	7.1890	0.2470
0.5000	7.8663	7.8756	0.1172
0.7514	8.3134	8.3044	0.1076
1.0037	8.6338	8.6180	0.1824
1.2550	8.8495	8.8619	0.1398

20 degrees

Velocity	Voltage	Vc	% Error
0.0000	3.6043	3.6052	0.0233
0.1218	6.5899	6.5827	0.0947
0.2481	7.1681	7.1672	0.0100
0.4991	7.8066	7.8278	0.2721
0.7516	8.2573	8.2536	0.0450
1.0039	8.5998	8.5707	0.3382
1.2549	8.8053	8.8232	0.2029

30 degrees

Velocity	Voltage	Vc	% Error
0.0000	3.5720	3.5723	0.0085
0.1215	6.5628	6.5545	0.1236
0.2484	7.0791	7.0874	0.1175
0.4996	7.7335	7.7377	0.0542
0.7510	8.1679	8.1905	0.2760
1.0031	8.6066	8.5508	0.6495
1.2552	8.8254	8.8543	0.3280

40 degrees

Velocity	Voltage	Vc	% Error
0.0000	3.6081	3.6095	0.0377
0.1222	6.6124	6.5958	0.2477
0.2481	7.1513	7.1628	0.1595
0.4994	7.7815	7.8125	0.3986
0.7518	8.2530	8.2362	0.2045
1.0038	8.5924	8.5553	0.4325
1.2553	8.7863	8.8133	0.3073

Table 7 : Pitch Calibration (S2)

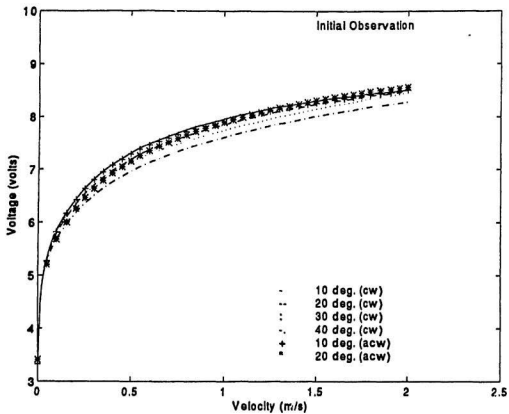


Fig. 11 : Effect of Varied Pitch Angle (S3)*

* Initial observation during the burn in period.

Velocity	Voltage	Vc	% Error
0.0000	3.3165	3.3166	0.0018
0.1219	5.9961	6.0037	0.1338
0.2478	6.6577	6.6305	0.4107
0.4993	7.2570	7.2993	0.5791
0.7514	7.6984	7.6922	0.0815
1.0028	7.9932	7.9595	0.4214
1.2543	8.1542	8.1546	0.0061
1.5061	8.2872	8.3022	0.1826
1.8092	8.4163	8.4357	0.2305
2.0087	8.5210	8.5037	0.2044

Velocity	Voltage	Vc	% Error
0.0000	3.3299	3.3297	0.0101
0.1218	5.9286	5.9357	0.1255
0.2480	6.5462	6.5317	0.2228
0.5003	7.1838	7.1826	0.0193
0.7513	7.5407	7.5761	0.4675
1.0039	7.8820	7.8564	0.3241
1.2549	8.0851	8.0681	0.2088
1.5071	8.2281	8.2364	0.1024
1.8086	8.3748	8.3966	0.2607
2.0100	8.4988	8.4849	0.1652

Velocity	Voltage	Vc	% Error
0.0000	3.2985	3.3002	0.0474
0.1212	5.9807	5.9612	0.3184
0.2476	6.5002	6.5227	0.3430
0.4996	7.0906	7.1184	0.3878
0.7509	7.5252	7.4814	0.5835
1.0028	7.7605	7.7488	0.1497
1.2551	7.9464	7.9647	0.2323
1.5064	8.1512	8.1483	0.0331
1.8083	8.3073	8.3426	0.4252
2.0093	8.4882	8.4611	0.3216

Velocity	Voltage	Vc	% Error
0.0000	3.3426	3.3444	0.0537
0.1216	5.8296	5.8122	0.2989
0.2475	6.3406	6.3476	0.1112
0.4995	6.9003	6.9541	0.7796
0.7507	7.3731	7.3353	0.5113
1.0033	7.6560	7.6151	0.5337
1.2542	7.8197	7.8325	0.1635
1.5062	7.9907	8.0101	0.2427
1.8080	8.1553	8.1847	0.3609
2.0089	8.3109	8.2835	0.3297

Velocity	Voltage	Vc	% Error
0.0000	3.3254	3.3278	0.0667
0.1208	6.0073	5.9701	0.6111
0.2475	6.5531	6.6189	1.0036
0.4994	7.2693	7.2823	0.1745
0.7511	7.7938	7.6590	1.7316
1.0031	7.8650	7.9153	0.6404
1.2540	7.9848	8.1067	1.5286
1.5053	8.2976	8.2608	0.4418
1.8069	8.5205	8.4158	1.2279
2.0083	8.4443	8.5082	0.7542

Velocity	Voltage	Vc	% Error
0.0000	3.3943	3.4112	0.4936
0.1220	5.8560	5.8335	0.3830
0.2475	6.5217	6.4475	1.1375
0.5002	7.0651	7.1521	1.2310
0.7520	7.4537	7.5881	1.8027
1.0043	7.9769	7.8979	0.9904
1.2551	8.2464	8.1292	1.4216
1.5075	8.2891	8.3089	0.2382
1.8092	8.4424	8.4727	0.3588
2.0101	8.5469	8.5578	0.1275

Table 8 : Pitch calibration (S3)*

* Initial calibration during the burn in period.

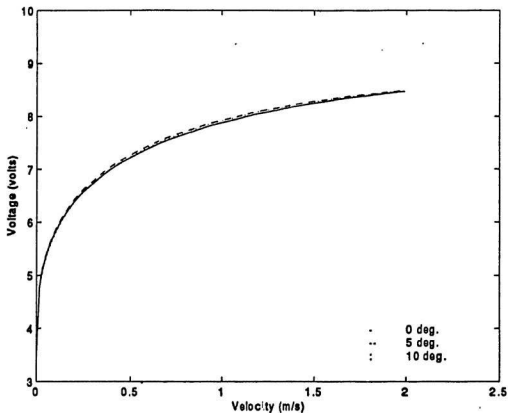


Fig. 12 : Effect of Varied Pitch Angle (S3)*

* After the sensor had stabilized.

Normal

Velocity	Voltage	Vc	% Error
0.0000	3.4336	3.4349	0.0373
0.1211	6.0005	5.9956	0.0815
0.2476	6.5697	6.5724	0.0406
0.7515	7.6078	7.6007	0.0933
1.0032	7.8514	7.8760	0.3133
1.5062	8.2702	8.2435	0.3228
2.0088	8.4614	8.4718	0.1234

5 degrees

Velocity	Voltage	Vc	% Error
0.0000	3.4336	3.4413	0.2218
0.1113	6.0074	5.9633	0.7334
0.2480	6.5713	6.6146	0.6591
0.7512	7.6223	7.6488	0.3471
1.0026	7.9547	7.9208	0.4262
1.5061	8.2854	8.2764	0.1089
2.0094	8.4761	8.4871	0.1305

10 degrees

Velocity	Voltage	Vc	% Error
0.0000	3.4336	3.4355	0.0545
0.1213	5.9654	5.9678	0.0415
0.2472	6.5792	6.5641	0.2302
0.7518	7.6054	7.6306	0.3317
1.0032	7.9069	7.9101	0.0401
1.5065	8.3044	8.2727	0.3815
2.0087	8.4682	8.4828	0.1723

Table 9 : Pitch Calibration (S3)*

* After the sensor had stabilized.

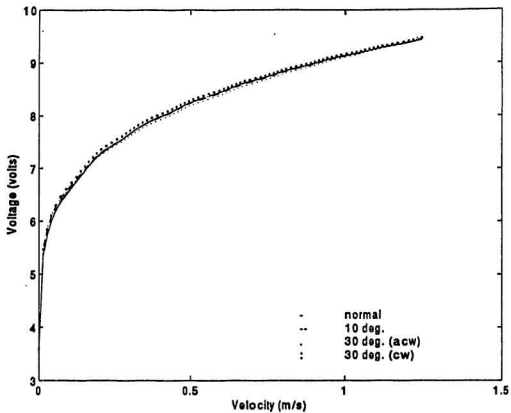


Fig. 13 : Effect of Varied Pitch Angle (S5)

Normal

Velocity	Voltage	Vc	% Error
0.0000	3.5922	3.5947	0.0693
0.1215	6.7793	6.7579	0.3145
0.2485	7.4292	7.4453	0.2162
0.5005	8.2039	8.2346	0.3736
0.7518	8.7656	8.7475	0.2073
1.0040	9.1695	9.1354	0.3719
1.2555	9.4226	9.4475	0.2645

10 degrees (ACW)

Velocity	Voltage	Vc	% Error
0.0000	3.6173	3.6176	0.0088
0.1215	6.8015	6.8013	0.0028
0.2480	7.4584	7.4514	0.0939
0.4999	8.2038	8.2178	0.1700
0.7514	8.7213	8.7308	0.1085
1.0035	9.1617	9.1287	0.3604
1.2542	9.4393	9.4560	0.1766

30 degrees (ACW)

Velocity	Voltage	Vc	% Error
0.0000	3.5904	3.5909	0.0134
0.1228	6.8575	6.8550	0.0357
0.2486	7.5140	7.5090	0.0688
0.5003	8.2517	8.2735	0.2640
0.7517	8.7879	8.7772	0.1223
1.0039	9.1777	9.1629	0.1611
1.2546	9.4656	9.4764	0.1146

30 degrees (CW)

Velocity	Voltage	Vc	% Error
0.0000	3.5904	3.5906	0.0083
0.1213	6.7807	6.7794	0.0192
0.2485	7.4255	7.4166	0.1199
0.4991	8.1551	8.1763	0.2602
0.7514	8.6793	8.6991	0.2276
1.0030	9.1702	9.1074	0.6853
1.2547	9.4162	9.4484	0.3417

Table 10 : Pitch Calibration (S5)

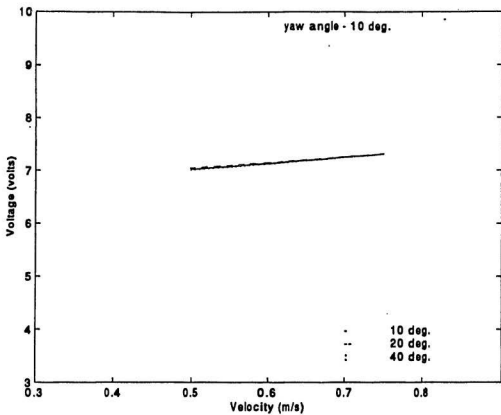


Fig. 14 : Yaw-Pitch Calibration (S3)*

* Fixed yaw angle of 10° and varied pitch angle.

10 degrees

Velocity	Voltage
0.4953	7.0163
0.7517	7.3044

20 degrees

Velocity	Voltage
0.4986	7.0381
0.7512	7.3043

40 degrees

Velocity	Voltage
0.4995	6.9981
0.7509	7.3001

Table 11 : Yaw-Pitch Calibration (S3)*

* Fixed yaw angle of 10° and varied pitch angle.

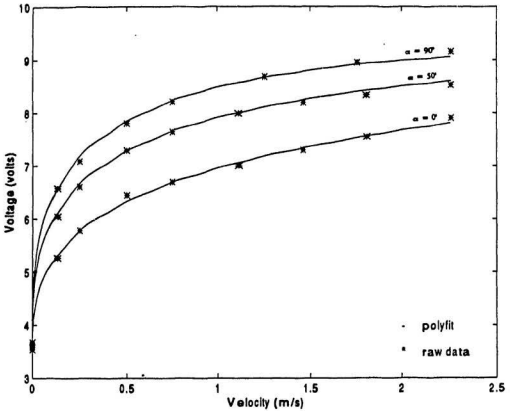


Fig. 15 : Yaw Calibration (S1)*

* Yaw calibration was also done at 80° , 70° , 60° , 30° , 20° and 10° .

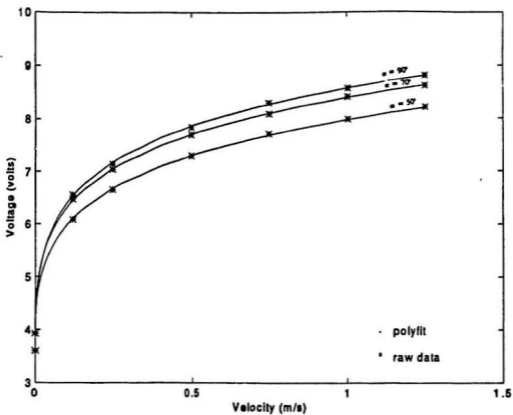


Fig. 16 : Yaw Calibration (S2)*

* Yaw calibration was also done at 80° and 60°.

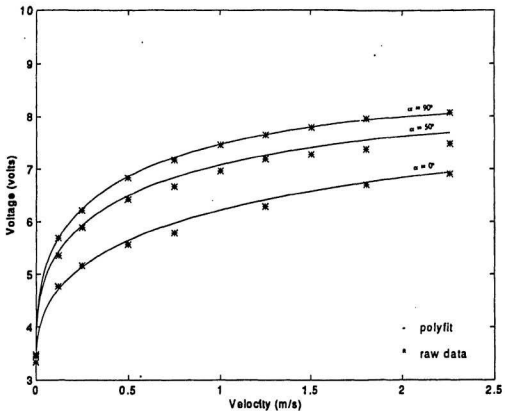


Fig. 17 : Yaw Calibration (S3)*

* Yaw calibration was also done at 80° , 70° , 60° , 30° , 20° and 10° .

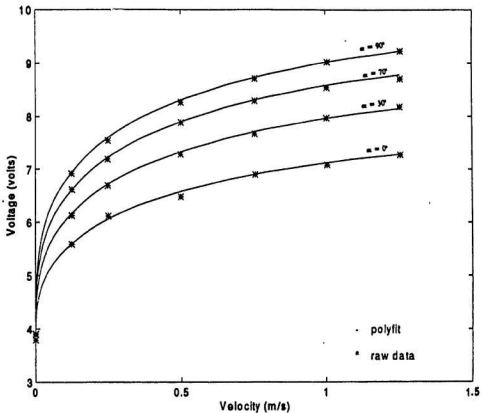


Fig. 18 : Yaw Calibration (S5)*

* Yaw calibration was also done at 80°, 60°, 20° and 10°.

CHAPTER FOUR

Wake Survey Using CTA

Wake survey, in general, is conducted on ship models to clearly quantify the flow pattern in the propeller plane. The nature of the flow in the wake governs the design of an efficient propulsion and steering system. Also, the pattern of flow behind the hull will be influenced by the basic hull form and will determine the selection and placement of propulsors. The wake behind a ship model is complex and three-dimensional. A theoretical approach to its determination is not generally pursued. However, with the advent of supercomputers, a computational approach could become feasible in the near future. An analytical approach requires the clear interpretation of the flow, in addition to solving the Navier-Stokes equations in three dimensions at high Reynolds' numbers. The most practical method for wake determination, which has been followed to date, is to carry out experiments on a model and extrapolate the results to that of a full scale ship. Tests on a full scale ship are expensive and not generally feasible.

Model nominal wake data for ships are presented either as a contour plot or as curves of velocity versus angular position and radii in the propeller plane.

4.1 Experimental Procedure

A model of a round bilge fishing vessel (M445) was used for this study. This model is similar to recent designs of long-liners in Newfoundland. Figure 19 is a body plan of the model and table 12 gives the model particulars. Pitot tube wake survey results at speeds of 0.54 m/s and 1.8 m/s were available for this model from previous tests done at the Institute for Marine Dynamics. These speeds were equivalent to full scale ship speeds of 3 knots and 9 knots respectively. The wake survey using hot film anemometry in this study was done at a speed of 0.55 m/s.

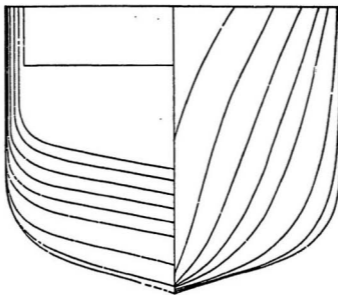


Fig. 19 : Body Plan of Round Bilge Model

Model/ShipScale	:	1 : 8
Length, BP	:	2.125 m
Breadth, Max	:	0.838 m
Draft, FP	:	0.396 m
Draft, AP	:	0.431 m
Trim	:	0.035 m
Displacement	:	0.438 Mt

Table 12 : Model Particulars

In this work, modifications were made to the wake rake that was used for the pitot tube wake survey in order to accommodate the 3-D hot film sensor. Figure 3 shows the configuration of the three sensors in a holder which was held in the wake rake. The rake unit and the associated sensor holder for wake survey is shown in figure 20.

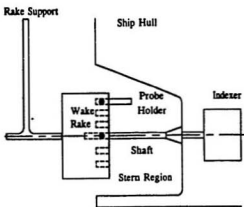


Fig. 20 : Wake Survey Setup

The rake unit, which could be rotated about the propeller shaft axis, accommodated the sensors at five different radii; each radius was on the propeller plane. The wake rake was rotated by a digitally controlled stepping motor fixed on the inboard end of the shaft. The top portion of the skeg near the region of the hull represented 0° and the bottom portion of the skeg in the region of the keel represented 180° . The entire wake rake unit was rotated in the clockwise direction (looking from the stern portion) which covered half the propeller plane. Each sensor, in the 3-D setup, was connected by standard cables to three anemometers which helped maintain a constant overheat ratio of 0.4 throughout the test. The response of the three sensors in the wake of the model was sampled at 300 Hz for a sampling period of 20 seconds. Data of carriage speed and sensor output were recorded on a computer through a Keithley 575 16 bit A/D convertor. Tests were done over a period of five days (one radius per day). Calibration of sensors were done every morning and the actual tests were done in the afternoon.

4.2 Wake Survey Results

Test voltages from the three sensors contained velocities and directions. As a result, an iterative approach was adopted to determine the velocity and direction of flow (with respect to each sensor). The coefficients of the two-variable non-linear polynomial (one set for each sensor) and test voltages were put through an iterative program to solve for axial, tangential and radial components of velocities. The routine of the program was

to assume a velocity close to the free stream velocity, iterate for the yaw angle of each sensor and substitute each yaw angle in the direction cosine relation for the respective sensor. From the three components of velocities, thus obtained, the modulus was calculated and compared with the assumed velocity. The process was repeated till the assumed velocity almost equalled the calculated velocity. Subsequently, the three components of velocities were transformed into vessel coordinates. This iterative program was successfully tested for known values of voltage, velocity and yaw angle which were obtained from the yaw calibration process. The program used for iteration is available in the appendix.

Results from the pitot tube wake survey are presented in the following pages [Nordco Ltd. (1991)]. Figures 21, 22 and 23 represent axial, tangential and radial components of velocities in the wake, at a model test speed of 0.54 m/s and 5 radii along the propeller plane. Test results were available for the entire region of the propeller plane (0° to 360°). Assuming symmetrical flow on either sides of the propeller plane, CTA wake survey was done on one half of the propeller plane (0° to 180° , clockwise direction, looking from the stern).

Wake survey results using constant temperature anemometers are presented in figures 24, 25 and 26. The variation in the pattern of the flow over the five day test period is either due to varying temperatures during the test period or deterioration of sensors after prolonged use. Temperature variation during the entire test period was found

to be $\pm 0.5^{\circ}\text{C}$. In the region of 50° to 150° , the sensors were exposed to the free stream flow and as a result should measure the free stream velocity. The reduction and variation in the axial component in this range (fig. 24) shows that the temperature correction based on calibrations done on the respective days of the test needs to be improved. Based on the calibration done every day before the test, the test data was approximated linearly (with 0.55 m/s as the reference, a multiplication factor was established). Figures 25 and 26 represent the tangential and radial component of velocities. The pattern is comparable to that of the pitot tube wake survey results. The amount of reduction in the axial component of velocity tends to augment the tangential and radial velocity components due to the geometry used in the iteration process.

Both wake surveys confirm a relatively uniform distribution of water flow in the propeller plane for angles ranging from 50° to 150° , except for the region of skeg. The drop in the axial velocity component in the region of skeg is due to the flow retardation generated by the presence of the skeg.

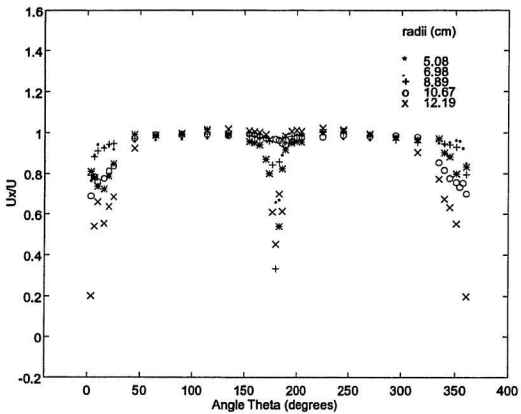


Fig. 21 : Pitot Tube Wake Survey (axial velocity)

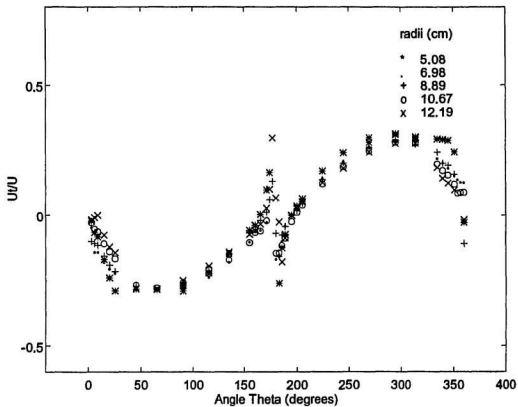


Fig. 22 : Pitot Tube Wake Survey (tangential velocity)

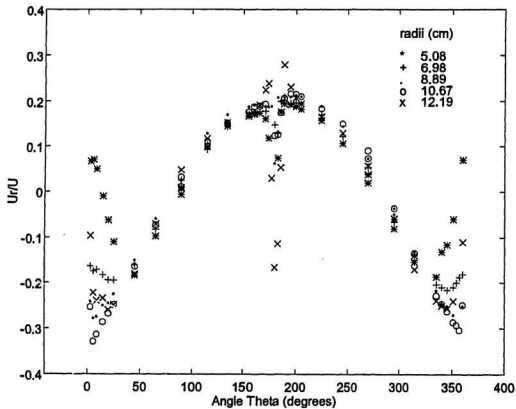


Fig. 23 : Pitot Tube Wake Survey (radial velocity)

deg.	Ux/U	Ut/U	Ur/U
3	0.81051	-0.02297	0.06689
6	0.78138	-0.06613	0.07136
9	0.73743	-0.08159	0.05034
15	0.72309	-0.16840	-0.00966
20	0.78707	-0.23801	-0.06155
25	0.84996	-0.28862	-0.11024
45	0.99080	-0.28177	-0.18527
65	0.98620	-0.28412	-0.09679
90	0.99442	-0.26940	0.00890
115	1.01502	-0.21902	0.09802
135	0.99415	-0.14480	0.14415
155	0.95690	-0.05742	0.16632
160	0.95119	-0.03785	0.17012
165	0.94132	0.00290	0.17359
171	0.87107	0.09595	0.16127
183	0.53912	-0.25827	0.07403
186	0.82341	-0.12403	0.17563
189	0.91676	-0.07252	0.19446
195	0.94892	0.00002	0.19244
200	0.95632	0.03522	0.18783
205	0.95460	0.06299	0.18240
225	1.00158	0.16831	0.15683
245	1.00697	0.23906	0.10954
270	0.99048	0.29843	0.01954
295	0.97812	0.31441	-0.07970
315	0.96706	0.29843	-0.15379
335	0.96982	0.29311	-0.18682
340	0.90235	0.29109	-0.13063
345	0.88442	0.28701	-0.11490
351	0.79888	0.24150	-0.05991
360	0.83349	-0.02708	0.07032

Table 13 : Pitot Tube Wake Survey Data (radius - 5.08 cm)

deg.	Ux/U	Ut/U	Ur/U
3	0.76378	-0.04849	-0.16367
6	0.88961	-0.14200	-0.17470
9	0.94227	-0.14218	-0.17183
15	0.93106	-0.17918	-0.18427
20	0.93731	-0.20452	-0.19521
25	0.92012	-0.22003	-0.19571
45	0.95727	-0.27469	-0.16189
65	0.96402	-0.28769	-0.08184
90	0.96819	-0.26759	0.02453
115	0.97281	-0.21604	0.10544
135	0.98704	-0.17757	0.14188
155	1.00161	-0.10321	0.17186
160	0.99947	-0.06380	0.17648
165	0.99135	-0.05702	0.17627
171	0.98288	-0.02797	0.17818
183	0.66769	-0.15756	0.12762
186	0.89171	-0.10111	0.19854
189	0.94831	-0.04247	0.20920
195	0.96548	0.00018	0.19542
200	0.98746	0.02523	0.19640
205	0.98724	0.05108	0.19384
225	0.99365	0.13901	0.16863
245	0.97065	0.20531	0.12061
270	0.96432	0.26147	0.03950
295	0.96628	0.28222	-0.06583
315	0.95817	0.26667	-0.14882
335	0.94873	0.21585	-0.20404
340	0.94173	0.19765	-0.20974
345	0.95186	0.17823	-0.21577
351	0.96234	0.15001	-0.21045
360	0.85014	0.12279	-0.18059

Table 14 : Pitot Tube Wake Survey Data (radius - 6.98 cm)

deg.	Ux/U	Ut/U	Ur/U
3	0.79088	-0.10025	-0.24162
6	0.88392	-0.10695	-0.27823
9	0.91180	-0.11430	-0.27459
15	0.92633	-0.15530	-0.25086
20	0.94332	-0.18899	-0.24645
25	0.94707	-0.21386	-0.22625
45	0.97085	-0.27191	-0.15129
65	0.97702	-0.28546	-0.05866
90	0.98664	-0.26463	0.04740
115	0.99390	-0.21135	0.12764
135	0.99846	-0.14806	0.16940
155	0.98812	-0.06561	0.18663
160	0.98215	-0.04476	0.19083
165	0.97652	-0.02033	0.18729
171	0.97360	0.01218	0.18820
183	0.85926	-0.15564	0.20825
186	0.97060	-0.07602	0.20021
189	0.97819	-0.04282	0.20258
195	0.98133	-0.00985	0.20932
200	0.98499	0.01739	0.21309
205	0.98248	0.04490	0.20951
225	1.00301	0.13594	0.18770
245	0.99776	0.19948	0.14255
270	0.98095	0.26123	0.05959
295	0.96404	0.28487	-0.04938
315	0.95240	0.27051	-0.13772
335	0.96232	0.24129	-0.21836
340	0.94545	0.19778	-0.24545
345	0.94038	0.19028	-0.25213
351	0.92993	0.15621	-0.27084
360	0.79561	-0.10650	-0.25190

Table 15 : Pitot Tube Wake Survey Data (radius - 8.89 cm)

deg.	Ux/U	Ut/U	Ur/U
3	0.68804	-0.02877	-0.25359
6	0.78367	-0.05356	-0.32948
9	0.75911	-0.06275	-0.31445
15	0.77536	-0.10840	-0.28693
20	0.81179	-0.13861	-0.26770
25	0.83668	-0.16483	-0.24850
45	0.97284	-0.26666	-0.16542
65	0.98914	-0.27832	-0.07278
90	0.98993	-0.25575	0.03199
115	0.99123	-0.20207	0.11133
135	0.98559	-0.14919	0.15095
155	0.99289	-0.10514	0.17645
160	0.98987	-0.06624	0.18676
165	0.98239	-0.06036	0.18781
171	0.97244	-0.02118	0.19297
183	0.96132	-0.14252	0.12487
186	0.94834	-0.11485	0.17400
189	0.94086	-0.08727	0.20662
195	0.95548	-0.02498	0.21571
200	0.97684	0.01140	0.21474
205	0.97808	0.03947	0.20954
225	0.97779	0.11804	0.18264
245	0.98637	0.18415	0.14889
270	0.98099	0.24534	0.07346
295	0.98461	0.28172	-0.03576
315	0.97794	0.27970	-0.13434
335	0.85417	0.19483	-0.22867
340	0.81571	0.16917	-0.24705
345	0.77477	0.15190	-0.26337
351	0.75534	0.11685	-0.28655
360	0.69842	0.08748	-0.24872

Table 16 : Pitot Tube Wake Survey Data (radius - 10.67 cm)

deg.	Ux/U	Ut/U	Ur/U
3	0.20152	-0.01750	-0.09561
6	0.53885	-0.00858	-0.22262
9	0.59540	-0.00143	-0.23957
15	0.55268	-0.07558	-0.23529
20	0.63538	-0.11973	-0.25975
25	0.68395	-0.14203	-0.24899
45	0.92452	-0.27783	-0.18141
65	0.98795	-0.28141	-0.07009
90	0.99573	-0.24942	0.04753
115	1.01054	-0.19242	0.11730
135	1.01823	-0.13867	0.15156
155	1.00901	-0.07294	0.17136
160	1.00520	-0.05781	0.17947
165	1.00164	-0.03285	0.19138
171	0.99131	0.02700	0.22535
183	0.69852	-0.02575	-0.11293
186	0.61364	-0.17661	0.05423
189	0.98377	-0.08569	0.28038
195	1.00671	-0.00160	0.23110
200	1.01138	0.02664	0.20735
205	1.00621	0.04899	0.19438
225	1.02249	0.12328	0.16454
245	1.01362	0.17877	0.12903
270	0.99409	0.24168	0.05663
295	0.97815	0.27645	-0.05829
315	0.90512	0.27739	-0.16985
335	0.77343	0.18318	-0.23936
340	0.67237	0.14001	-0.25067
345	0.63198	0.12169	-0.25726
351	0.55130	0.09599	-0.24065
360	0.19839	-0.01658	-0.10850

Table 17 : Pitot Tube Wake Survey Data (radius - 12.19 cm)

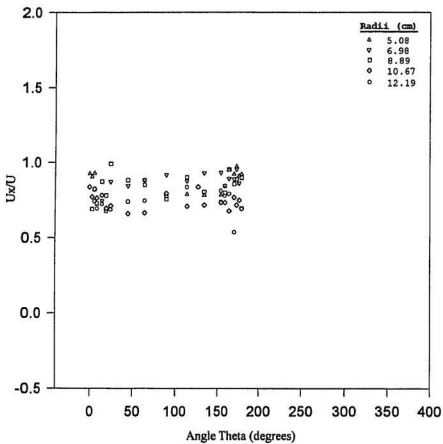


Fig. 24 : CTA Wake Survey (axial velocity)

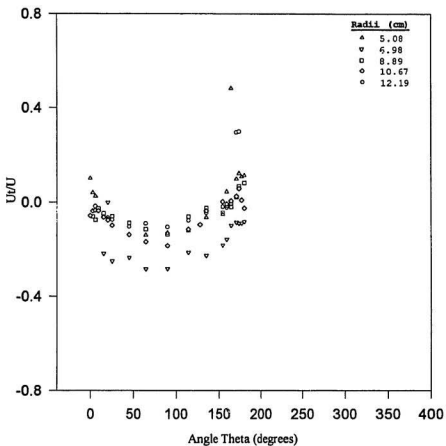


Fig. 25 : CTA Wake Survey (tangential velocity)

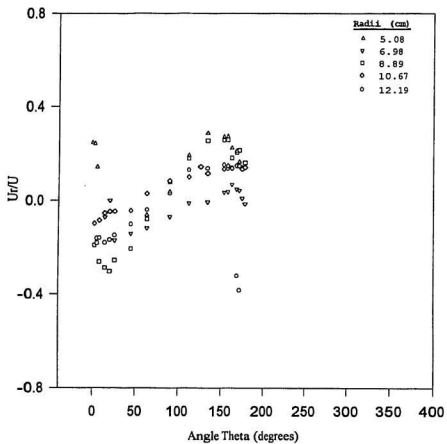


Fig. 26 : CTA Wake Survey (radial velocity)

4.3 Comparison of Results

Figures 27, 28 and 29 represent a comparison between wake survey data obtained using constant temperature anemometers and pitot tubes. The wake pattern at a radius of 12.19 cm along the propeller plane, established by these two methods, has been compared.

Wake survey done using both CTA and pitot tubes indicate a relatively uniform flow in the region of 60° to 170° (fig. 27). The lower values of the axial component of velocity in this region, using CTA, can be attributed to problems associated with temperature correction. In this range, the sensors were exposed to the free stream flow and hence should have predicted the test speed of 0.55 m/s. In the region of the bottom portion of the skeg (around 180°), there is a drop in the axial velocity component, as observed by both methods. Turbulence in this region resulted in an increase in the tangential velocity component (fig. 28). In the range of 0° to 30° (skeg portion near the hull), the CTA method indicates more or less a smooth flow as compared to pitot tube wake survey; which is due to an ambiguity in the water line length and the model displacement indicated in the pitot tube wake survey report [Nordco Ltd. (1991)]. Another indication of CTA measuring more axial and uniform flow in that region can be seen in figure 28; where the tangential velocity components are smaller in magnitude as compared to pitot tube wake survey. A similar trend is also observed in figure 29; which represents radial velocity component in the range of 0° to 180° .

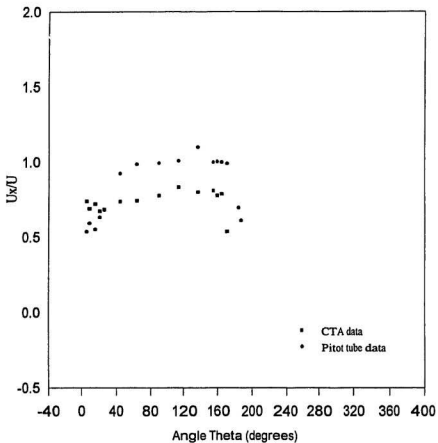


Fig. 27 : Comparison of Axial Velocity Component (radius - 12.19 cm)

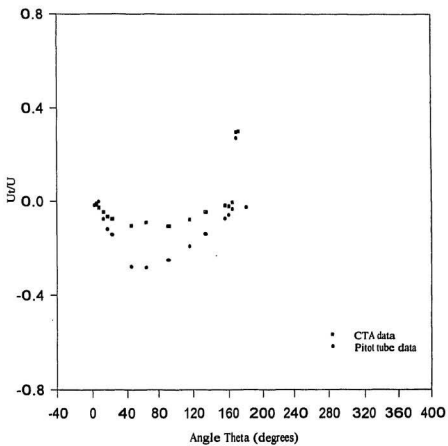


Fig. 28 : Comparison of Tangential Velocity Component (radius - 12.19 cm)

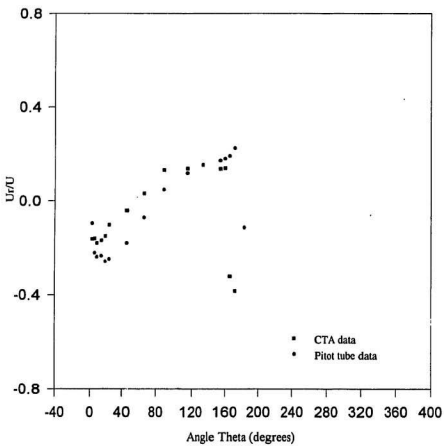


Fig. 29 : Comparison of Radial Velocity Component (radius - 12.19 cm)

4.4 Level and Frequency of Turbulence

The intensity of turbulence can be represented by its energy spectrum over the turbulence frequency range. To analyze the frequency components of turbulence, a fast Fourier transform (FFT) was performed on the time-domain recording of converted velocities (values obtained after iteration). During the iteration process, some of the test data in the close vicinity of the skeg showed signs of flow reversal. This is indicative of the turbulent nature of flow in the propeller plane. For practical purposes, turbulence can be regarded as having frequencies below 45-50Hz. The sampling frequency is normally ten times that of the maximum turbulence frequency of interest. By considering the turbulence to be mostly under 30Hz from the present results, a sampling rate of 300Hz was chosen.

Typical energy spectra of the recording at various radii and angular positions are shown in figures 30, 31 and 32. Figure 30 indicates the presence of maximum turbulence in the region of skeg (near the keel), at a dominant frequency of approximately 13Hz. Figure 31 represents the energy content at radii of 5.08 cm and 10.67 cm along the radial line of 90°. It can be seen that the dominant frequency occurs at a very low frequency of approximately 2Hz and the lower energy content clearly indicates lower levels of turbulence far away from the skeg. Figure 32 represents turbulence in the region of the skeg (near the hull) which appears to have decreasing

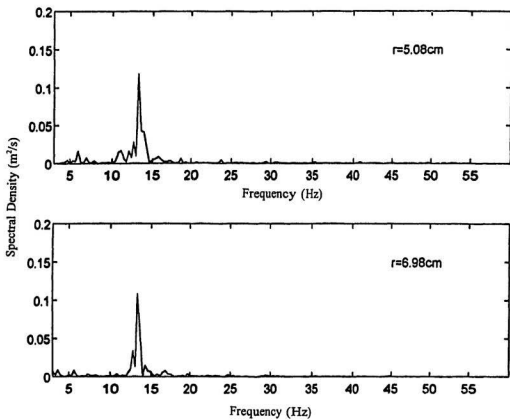


Fig. 30 : Spectral Analysis (160° radial line)

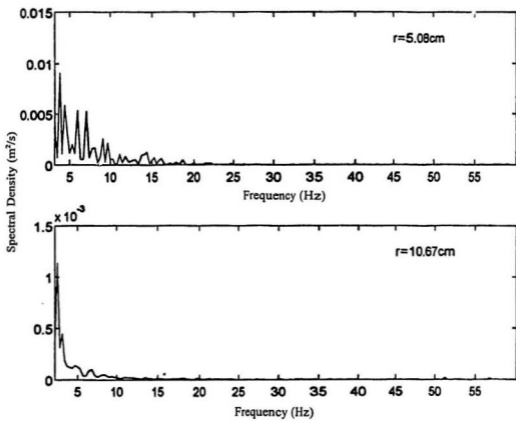


Fig. 31 : Spectral Analysis (90° radial line)

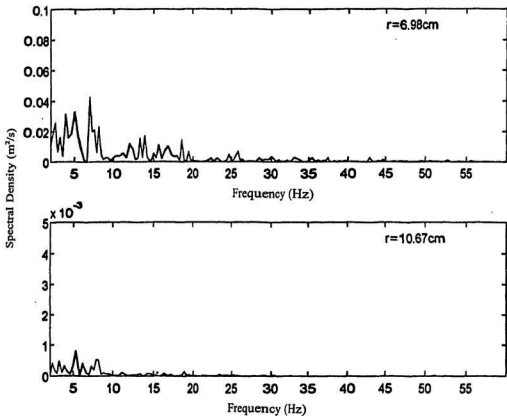


Fig. 32 : Spectral Analysis (15° radial line)

levels of turbulence at higher radii. Due to varying levels of turbulence, different scales have been used in these plots in order to identify the dominant frequency at one angular position and different radii.

The level of turbulence at the inner radius near the region of the skeg (along radial lines of 160° and 15°) is much higher than that for the outer radius. In the region of skeg (near the keel), a decrease in the axial component of velocity (fig. 24) and subsequent increase in tangential and radial components of velocity (fig. 25 and 26), indicates presence of turbulence in the region of skeg (near the keel). Along the radial direction of 90° , the energy content at radius of 6.98 cm is larger when compared to that at radius of 10.67 cm; which was mostly exposed to the free stream flow. Due to a relatively uniform distribution of water flowing into the propeller plane (except the region of skeg), the amount of energy in the spectrum is not significant and indicates that the level of turbulence is minimal.

Chapter Five

Discussion and Conclusions

All sensors were calibrated over a range of speeds. Prior to calibration of each sensor, the constant temperature anemometers were warmed up (at the beginning of the day) for nearly 90 minutes. This ensured thermal stability of the resistances in the electronic circuitry which otherwise would induce an error in measurements. Effects of humidity on the Wheatstone bridge balance were ignored.

Each sensor had to be put through a burn in period of approximately 70 - 80 hours before calibrations were done. Repeatability levels of normal calibrations were checked for individual sensors, which when curve fitted using the modified form of King's law showed their output to be stable. Pitch calibration was attempted on sensor 3; which during the initial stages appeared to be sensitive to changes in angles of pitch. However, sensor 3, once put through a further burn in period, demonstrated insensitivity to changes in angles of pitch. Pitch calibration was done for all sensors and data were curve fitted based on the modified King's law. It was concluded that the sensors were insensitive to changes in angles of pitch. A polynomial of 3rd order gave the best fit for both normal and pitch calibration data.

The directional sensitivity calibration, also commonly referred to as yaw calibration, covered yaw angles ranging from 0° to 90°. Yaw calibration data were curve fitted based on a two-variable non-linear polynomial of 3rd order. Yaw characteristics around 45° were interpolated based on the two-variable non-linear polynomial. In the region of interest (0.55 m/s), curve fitting error varied from 0.03 % to 1.5 %. Percentage error at each yaw calibration point is available in the Appendix.

The calibration velocity was measured with an accuracy of about ± 0.005 m/s [Bose and Luznik (1995)]. The entire calibration processes of all sensors were done at an overheat ratio of 0.4, which to a large extent eliminated the need for temperature correction. However, thermal currents were present in the wave tank which affected sensor response during the calibration process. The level of variation in temperature along the horizontal direction in the wave tank could not be measured continuously. Normal and pitch calibrations were done at a constant depth of 0.3 m (measured from the top surface of the water in the tank). However, yaw calibration was done at varying depths (in the top 0.3 m of water column) in the wave tank. On certain days, during the yaw calibration process, a temperature gradients of approximately $\pm 0.5^{\circ}\text{C}$ were observed in the top 0.3 m of water column. As this phenomenon was not observed continuously during the yaw calibration process, temperature correction was not applied to yaw calibration data. The complete effects of horizontal and vertical temperature gradients on sensor characteristics could not be accounted for by an appropriate

correction to the output of the sensors. Also, the thermal coefficient of expansion was assumed to be constant while calculating the decade resistance of the anemometer.

From the calibration plots it can be seen that, at high velocities, the gradient of the calibration curve is reduced compared with that at lower velocities. The calibration curve was flat at higher velocities, which indicated that the heat loss rate or the convection rate of the sensor had reached a limit and that the anemometer output voltage, V , became very insensitive to any further increase in velocity, U . Any test conducted in this range yields a large error in measured velocity, for the reason that any slight change in voltage, V , will correspond to a large change in velocity, U . Calibration at 0.55 m/s, which was our prime concern, fell in the highly non-linear range where the gradient of voltage against velocity was relatively large.

Results obtained from the pitot tube wake survey and this study indicate a relatively uniform axial distribution of flow in the propeller plane for angles from approximately 45° to 165° (i.e. with the exception of the skeg area). There is a large apparent scatter in the data obtained by this study which is due to the fact that the temperature varied within a range of $\pm 0.5^\circ\text{C}$ during the test period (five days). The pattern of flow was the same for all radii except for either a drop in velocity or an increase in velocity relative to one another (different radii). An improved temperature correction procedure will help eliminate the errors introduced by the linear approximation which was employed in this study. Also, there is a possibility that the sensors

deteriorated over the prolonged period in use. For instance, at a radius of 10.67 cm, which was done on the last day, there was a drop in the axial component of velocity when compared to tests done at other radii. However the pattern of flow appears to be unaffected. At all radii, there is an under prediction of the axial component of velocity which is due to inadequate temperature correction procedure. As a result, the radial and tangential components of velocity appear to be slightly higher when compared to the pitot tube wake survey. In addition, the testing region (described as the propeller plane) was not defined exactly in the pitot tube wake survey report. As a result, an assumption was made to locate the sensors midway between the skeg and the rudder line. Varied regions of testing could have caused non-conformity of results to some extent. However, this does not account for the variation of the data between different radii. A spectrum analysis along the propeller plane, (at various radii) indicates the presence of maximum energy content (level of turbulence) in the region of skeg and minimum energy content elsewhere.

To conclude, the study indicates that the measurements of flow velocity in three dimension, during nominal wake surveys in a towing tank, can be done using three inclined single hot film probes using constant temperature anemometry. However, the accuracy of results is limited due to two main factors :

1. Temperature variations occur in the disturbed flow behind a ship model and over the extent of a towing tank. At present, it is impractical to

continuously measure water temperature during a time series record and correct each data sample for the appropriate temperature. Here corrections were made based on calibrations done at the beginning of each day of tests. This overall correction for the general trend in the temperature variation in the tank was insufficient to maintain acceptable accuracy in the records.

2. The velocity components (axial, radial and tangential) were resolved from the three outputs from three single sensors. Any small variation in the accuracy of a signal (say that arising from an error in temperature correction) affects all three components of velocity.

To be a useful instrument for nominal wake survey, both these sources of error need to be addressed. This might be done by more reliable means for temperature correction, or it might be alleviated to some extent by use of a bank of sensors such that time changes between measurements are reduced. The latter would not account for spatial variation in temperature over the extent of the tank. The sensors do allow for relatively high spatial resolution in the measurement of velocity and for measurement of the energy levels contained in the turbulence. They are the only type of sensor which allow an effectively continuous signal to be made of velocity at a high frequency response.

References

- Bose, N. and Luznik, L., "Uncertainty analysis in propeller open water tests", Submitted to International Shipbuilding Progress, 1995.
- Champagne, F. H., Sleicher, C. A. and Wehrmann, O. H., "Turbulence measurements with inclined hot wire. Part I - heat transfer experiments with inclined hot wire.", Journal of Fluid Mech., vol.28, part 1, pp153-175, 1967.
- Disa Elektroniks, Inc., "Instruction and service manual for type 55M10 CTA", Disa Elektronik A/S.
- Durrani, S. Tariq, and Greated, A. Clive, "Laser Systems in Flow Measurement", Plenum Press, New York, 1977.
- Eric, W. Nelson and John, A. Borgos, "Dynamic response of conical and wedge type hot films: Comparison of experimental and theoretical results", TSI Incorporated, Vol. IX, Issue 1, January-March 1983.
- Fernando, E. M., Donovan, J. F. and Smits, A. J., "The calibration and operation of a constant-temperature crossed-wire probe in supersonic flow", Dept. of Mech. and Aero. Engg., Princeton Univ., New Jersey, 1988.
- Freymuth, Peter, "Review : A Bibliography of Thermal Anemometry", Transactions of the ASME, Vol. 102, June 1980.
- Harris, C. "A particle tracking system for wake survey", M. Engg. Thesis, Memorial University of Newfoundland, St. John's, Newfoundland, Canada, 1992.

- Hollasch, K. and Gebhart, B., "Calibration of constant-temperature hot-wire anemometers at low velocities in water with variable fluid temperature", ASME-AIChE Heat Transfer Conference, 1971.
- Jimenez, J., Martinez-Val, R. and Rebollo, M., "Hot-film sensors calibration drift in water", J. Phys. E. Sci. Instrumen., Vol. 14, 1981.
- Johnson, F. D. and Eckelmann, H., "A variable angle method of calibration for X-probes applied to wall-bounded turbulent shear flow", Experiments in Fluids 2, pp121-130, 1984.
- King, L. V., "On the convection of heat from small cylinders in a stream of fluid", phil. trans. Roy. Soc. London, Sec. A, Vol. 214, pp373-432, 1914.
- Lakshminarayana, B., "Three sensor hot wire/film technique for three dimensional mean and turbulence flow field measurement", Prepared for TSI Incorporated, Vol. VIII, Issue 1, January-March 1982.
- Lomas, G. Charles, "Fundamentals of Hot Wire Anemometry", Cambridge University Press, London, 1986.
- Morrow, T. B. and Kline, S. J., "The performance of hot-wire and hot-film anemometers used in water", Instrument Society of America, pp555-562, 1974.
- Mulhearn, P. and Finigan, J., "A device for dynamic testing of X-configuration hot-wire anemometer probes", J. Phys. E. Sci. Instrum., Vol. 11, 1978.
- Nordco Limited, "An investigation of the resistance, self-propulsion and seakeeping characteristics of two 65' fishing vessels", Report on work contracted by the Institute for Marine Dynamics, Project No. 143-90G, March 1991.

- Okuno, Taketoshi, "A note on the turbulence measurements by means of hot-film probes", Dept. of Naval Arch., College of Engg., Univ. of Osaka, Japan, 1988.
- Perry, A. E., "Hot-Wire Anemometry", Clarendon Press, Oxford, 1982.
- PrahI, J. M. and Win, H., "Calibration of constant-temperature hot-film anemometers at low velocities in water of uniform temperature", Int. Comm. Heat and Mass Transfer, Vol. 13, pp567-575, 1986.
- PrahI, J. M. and Win, H., "Calibration of constant-temperature hot-film anemometers at low velocities in water of varying temperature", Dept. of Mech. and Aero. Engg., Case Western Reserve University, Cleveland, Ohio, 1987.
- Rahman-Abdel, A., Tropea, C., Slawson, P. and Strong, A., "On temperature compensation in hot-wire anemometry", J. Phys. E. Sci. Instrum., Vol. 20, 1987.
- Resch, F. J., "Turbulence measurements in water", Proc. Symp. on Turbulence Measurements in Liquids, pp60-61, September 1969.
- Udo, R. Muller, "Measurement of the Reynolds stresses and the mean-flow field in a three-dimensional pressure-driven boundary layer", Journal of Fluid Mechanics, Vol. 119, pp121-153, 1982.
- Vukoslavcevic, P., Balint, J. L. and Wallace, J. M., "A multi-sensor hot-wire probe to measure vorticity and velocity in turbulent flows", Journal of Fluids Engg., Transactions of the ASME, Vol. 111, No. 2, pp220-224, June 1989.
- Watrasiewicz, B. M. and Rudd, M. J., "Laser Doppler Measurements", Butterworth and Co. (Publishers) Ltd., 1976.

- Wu, S. and Bose, N., "Calibration of a wedge-shaped vee hot-film probe in a towing tank", *Measurement Science and Technology*, Vol. 4, pp101-108, 1993.
- Wu, S. and Bose, N., "Axial wake survey behind a fishing vessel model using a wedge-shaped hot-film probe", *Kansai Soc. of Naval Arch.*, Japan, May 1992.
- Wu, S. and Bose, N., "An extended power law model for the calibration of hot wire/hot-film constant temperature probes", *International Journal of Heat and Mass Transfer*, Vol. 37, No. 3, pp437-442, 1994.

Bibliography

1. Arndt, R. E. A., Stefan, H. G., Farell, C. and Peterson, S. M., "Advancements in Aerodynamics, Fluid Mechanics and Hydraulics", ASCE, 1986.
2. Durst, F., Melling, A. and Whitelaw, J. H., "Principles and Practice of Laser-Doppler Anemometry", Academic Press Inc. (London) Ltd., 1976.
3. Dreyer, G. F., "Calibration of Hot-Film Sensors in a Towing Tank and Application to Quantitative Turbulence Measurements", A student paper presented to the Chesapeake Section of the Society of Naval Architects and Marine Engineers, U. S. Naval Academy, Annapolis, Maryland, March 1967.
4. Fox, J. A., "Introduction to Fluid Mechanics", McGraw-Hill Book Co., 1974.
5. Harvald, SV. AA., "Resistance and Propulsion of Ships", John Wiley and Sons Inc., 1983.
6. Jackson, R. Herring and James, C. McWilliams, "Lecture Notes on Turbulence", World Scientific Publishing Company Pte. Ltd., 1989.
7. Kreyszig, E., "Advanced Engineering Mathematics", Fourth edition, John Wiley and Sons Inc., 1979.
8. Massey, B. S., "Mechanics of Fluids", Van Nostrand Co. Ltd., London, 1968.
9. Melnik, W. L. and Weske, J. R., "Advances in Hot-Wire Anemometry", AFOSR final report no. 68-1492, Dept. of Aero. Engg, Univ. of Maryland, July 1968.

10. Peerless, S. J., "Basic Fluid Mechanics", Pergamon Press Ltd., 1967.
11. Robert, P. Benedict, "Fundamentals of Temperature, Pressure and Flow Measurements", John Wiley and Sons Inc., 1969.
12. Rosenhead, L., "Laminar Boundary Layers", Oxford University Press, 1963.
13. Saad, A. M., "Compressible Fluid Flow", Prentice-Hall Inc., New Jersey, 1985.
14. Smol'yakov, A. V. and Tkachenko, V. M., "The measurement of Turbulent Fluctuations - An Introduction to Hot-Wire Anemometry and Related Transducers", Springer-Vestlag, New York, 1983.
15. Wu, S. and Bose, N., "Adoption of the DISA 55D05 CTA for Wake Measurements in the Towing Tank", OERC91-WTT-TR002, Memorial University of Newfoundland, Canada, June 1991.
16. Wu, S. and Bose, N., "Methods of Fitting Calibration Curves to Hot Film/Hot Wire Constant Temperature Anemometer Data", OERC91-WTT-TR003, Memorial University of Newfoundland, Canada, June 1991.
17. Wu, S. and Bose, N., "A Wedge-Shaped Vee Hot-Film Probe Calibrated for Towing Tank Measurements", OERC91-WTT-TR004, Memorial University of Newfoundland, Canada, June 1991.
18. Wu, S. and Bose, N., "Methods of Calibrating X-Wire Signals from Constant Temperature Anemometers", OERC91-WTT-TR005, Memorial University of Newfoundland, Canada, June 1991.

Appendix

- * Program to examine repeatability of normal and pitch calibration of sensors based on the modified form of King's law.
- * Program to evaluate the coefficients of two-variable non-linear polynomial based on yaw calibration data.
- * Input and output files of yaw calibration (from the above referred program).
- * Program to iterate values of velocity and yaw angle for a given voltage (used to analyze wake survey data).

Program to ensure repeatability of normal and pitch calibration of sensors

- Based on the modified form of King's law
- A 3rd order polynomial was used in this study
- Negligible curve fitting errors for repeated normal and pitch calibrations (presented in the body of this thesis) confirmed stability of the sensors. Subsequently, yaw calibrations were done.

```

C   THIS PROGRAM CURVE FITS DATA BASED ON THE VALUE OF M.
C   KING'S LAW WHEN M = 1 AND OTHERWISE BECOMES MODIFIED
C   FORM OF KING'S LAW.
      program stpfit
      implicit real*8 (a-h,o-z)
      parameter(numax = 100,namax = 11)
      dimension u(numax),v(numax),x(numax),y(numax),erxy(numax)
      dimension a(namax),b(namax),coef(namax,namax),cu(namax)
      common /acom/nx,ux(100),vx(100)
      COMMON /bout/mord
      character*15 file
      external xyfit,trans,fabn,dif,npoly,cyawkt

      open(2,file='input.dat',status='old')
      open(9,file='output.dat',status='new')

C   INPUT DATA IS FROM INPUT.DAT
C   OUTPUT IS STORED IN OUTPUT.DAT

C   ORDERING OF U.

C   NX - NUMBER OF CALIBRATION POINTS
      read(2,*) nx
C   READ IN VELOCITIES
      read(2,*) (ux(it),it=1,nx)
C   READ IN VOLTAGES
      read(2,*) (vx(it),it=1,nx)
      np = nx
      do 5 it = 1,numax
      u(it) = ux(it)
5     v(it) = vx(it)
      WRITE(5,*) (VX(IP),IP=1,NP)
      WRITE(5,*) (V(IP),IP=1,NP)
      DO 120 K = 1,NP-1
      DO 130 I = K + 1,NP
      IF(u(I).GE.u(K)) GOTO 130
      tr1 = u(K)
      u(K) = u(I)
      u(I) = tr1
      tr1 = v(K)
      v(K) = v(I)
      v(I) = tr1
130  CONTINUE
120  CONTINUE
      write(5,11)
11   format(1x,'input m as defined in Eq. (5)')
      read(5,*) mord
      mord = mord + 1

```

```

call npoly(c,u,v,np,cn,tse,tseod,mo,erxy)
write(9,51) np,(u(i),i=1,np)
write(9,61) (v(i),i=1,np)
51 format(1x,'data file ERRXY.DAT-output from STPFIT'
1 /1x,'number of calibration points np=' ,i5
1 //1x,'calibration velocities:',17(/1x,6f10.4))
61 format(1x,'calibration voltage output:',17(/1x,6f10.4))
mord=mord-1
write(9,21) mord,c,(cn(it),it=1,mo)
write(9,31) tseod,tse
21 format(1x,'order m=' ,i4
1 /1x,'exponent n=' ,f10.4
1 /1x,'coef. Ak=' ,5f13.6//10x,5f13.6)
31 format(1x,'error function E_1(V)=' ,e12.3
1 /1x,'error function E_2(V)=' ,e12.3//)
write(9,41) (erxy(ik),ik=1,np)
41 format(1x,'fit error at each point in %',17(/1x,6f10.4))
write(5,*) 'need to calculate the yaw factor? (1)'
read(5,*) nyes
if(nyes.eq.0) goto 999
write(5,*) (cn(it),it=1,mo)
call cyawkt(cn,mo,c)
999 continue
stop
end
subroutine npoly(c,u,v,np,cn,tse,tseod,mo,erxy)
implicit real*8 (a-h,o-z)
parameter(numax=100,namax=10)
dimension u(np),v(np),x(numax),y(numax),cn(namax+1)
dimension a(namax+1),coef(namax+1,namax+1),erxy(numax)
c0=0.2
cod=c0
c=c0
tc=c0
call fabn(tc,u,v,np,cn,tse0,tseod,mo,erxy)
do 20 i=1,60
tc=c0+0.01*i
call fabn(tc,u,v,np,a,tse,tseod,mo,erxy)
write(5,*) tc,tse,tseod,c,tse0
if(tse.ge.tse0) goto 20
c=tc
tse0=tse
do 25 it=1,mo
25 cn(it)=a(it)
20 continue
cc=c
do 30 i=1,10
tc=cc+0.001*i

```

```

    call fabn(tc,u,v,np,a,tse,tseod,mo,erxy)
    if(tse.ge.tse0) goto 40
    c=tc
    tse0=tse
    do 45 it=1,mo
45   cn(it)=a(it)
40   continue
    tc=cc-0.001*i
    call fabn(tc,u,v,np,a,tse,tseod,mo,erxy)
    if(tse.ge.tse0) goto 30
    c=tc
    tse0=tse
    do 35 it=1,mo
35   cn(it)=a(it)
30   continue
    cc=c
    do 50 i=1,10
    tc=cc+0.0001*i
    call fabn(tc,u,v,np,a,tse,tseod,mo,erxy)
    if(tse.ge.tse0) goto 60
    c=tc
    tse0=tse
    do 55 it=1,mo
55   cn(it)=a(it)
60   continue
    tc=cc-0.0001*i
    call fabn(tc,u,v,np,a,tse,tseod,mo,erxy)
    if(tse.ge.tse0) goto 50
    c=tc
    tse0=tse
    do 65 it=1,mo
65   cn(it)=a(it)
50   continue
    return
    end
    subroutine fabn(ex,u,v,np,a,tse,tseod,mo,erxy)
    implicit real*8 (a-h,o-z)
    parameter(numax=100,namax=10)
    dimension u(np),v(np),x(numax),y(numax)
    dimension a(namax+1),c(namax+1,namax+1),erxy(numax)
    call trans(ex,u,v,np,x,y,mo)
    call xyfit(x,y,np,mo,a,c,tse,var,erxy)
    tseod=0.
    do 10 i=1,np
    vfit=dif(a,mo,x(i),0.)
    if(vfit.le.0.) vfit=0.
    tseod=tseod+(v(i)-sqrt(vfit))**2
    erxy(i)=abs(v(i)-sqrt(vfit))/v(i)*100.

```

```

10  continue
C   gt=tse
C   tse=tseod
C   tseod=gt
    return
    end
    subroutine trans(ex,u,v,np,x,y,mo)
    implicit real*8 (a-h,o-z)
    common/hout/mord
    dimension u(np),v(np),x(np),y(np)
    mo=mord
    do 10 l=1,np
    x(l)=u(l)**ex
    y(l)=v(l)**2
10  continue
    return
    end

C
SUBROUTINE XYFIT(X,Y,NP,MO,A,C,TSE,VAR,ERXY)
implicit real*8 (a-h,o-z)
parameter(namax=10)
DIMENSION X(NP),Y(NP),ERXY(NP),A(MO),C(MO,MO),B(namax+1)
C NP:No. of data points
C MO-1: order of the polynomial (MO<=11 is set in the program)
N1=1
N2=NP
N=N2-N1+1
IF(MO.LE.11) GOTO 110
WRITE(5,120)
120 FORMAT(1X,'THE HIGHEST ORDER OF THE POLYNOMIAL < =10'
1 /1X,'RESTART WITH A LOWER NUMBER')
110 CONTINUE
XM=0.
YM=0.
DO 10 l=1,NP
XM=XM+X(l)
YM=YM+Y(l)
10 CONTINUE
XM=XM/NP
YM=YM/NP
DO 100 JO=1,MO
J=JO-1
XYB=0.
DO 200 l=N1,N2
XPART=1
IF(ABS(X(l))+J.GT.0) XPART=X(l)**J
200 XYB=XYB+Y(l)*XPART
B(JO)=XYB/NP

```

```

DO 300 KO=1,MO
K=KO-1
XB=0.
DO 400 I=N1,N2
XPART=1
IF(ABS(X(I))+J+K.GT.0) XPART=X(I)**(K+J)
400 XB=XB+XPART
300 C(J,O,KO)=XB/NP
100 CONTINUE

CALL DLSARG(MO,C,MO,B,1,A)
TSE=0.
VAR=0.
DO 500 I=N1,N2
SXY=0.
DO 600 K=1,MO
XPART=1
IF(ABS(X(I))+K-1.GT.0) XPART=X(I)**(K-1)
600 SXY=SXY+A(K)*XPART
C error in %
ERXY(I)=ABS(Y(I)-SXY)/ABS(Y(I))*100.
VAR=VAR+(Y(I)-YM)**2
500 TSE=TSE+(Y(I)-SXY)**2
RETURN
END
FUNCTION DIF(A,M,X,Y0)
implicit real*8 (a-h,o-z)
DIMENSION A(M)
C function DIF=F(x)-Y_0
C F(x) is a polynomial of x (M-1th order)
C A(M) are the coefficients
Y=0.
DO 10 I=1,M
IO=I-1
xpart=1
if(abs(x)+io.gt.0) xpart=x**io
10 Y=Y+A(I)*xpart
DIF=Y-Y0
RETURN
END
C calculation of the yaw factor
subroutine cyawkt(aco,mo,ex)
implicit real*8 (a-h,o-z)
parameter(namax=11,numax=100,pi=3.1415927/180.)
dimension aco(mo),yawf(numax,namax),yawkt(numax,namax)
dimension cmeanf(namax),crmsy(namax),xyma(namax),xymi(namax),
1 cmeank(namax),crmsk(namax),xkma(namax),xkmi(namax)
dimension u(numax,namax),v(numax,namax),nu(namax),ate(namax)

```

```

dimension erf(numax,namax),vc(numax,namax),suber(namax),
1 subrms(namax)
common /acom/nx,unorm(100),vnorm(100)
character*15 filen
data u,v/2200*0./
C statement function of the effective velocity
C du: the calibration velocity
C da: yaw angle (in radian)
C dkt: yaw factor
tra(da)=sin(da)
C ytra(da)=.1874269+3.222723e-3*tra(da)+1.02656227*
C 1 tra(da)**2-0.22411871*tra(da)**3
C ytra(da)=.207606+.313142*tra(da)+0.994339*tra(da)**2
C 1 -0.526574*tra(da)**3
C ytra(da)=0.150464+.118694*tra(da)+0.719069*tra(da)**2
C 1 +.324345e-2*tra(da)**3
C ytra(da)=0.207319-.0620522*tra(da)+2.0799*tra(da)**2
1 -1.21912*tra(da)**3
C cuef(du,da,dkt)=(du*ytra(da))**ex
C cuef(du,da,dkt)=(du*sqrt((sin(da))**2+
C 1 dkt**2*(cos(da))**2))**ex
C input data from channel 2
C input data file should be set up in the following format:
C 1st row: na - no. of yaw angle calibrations
C 2nd row: a_i - values of those yaw angles
C 3rd row: nuv_i - no. of velocity calibration at each
C corresponding yaw angle
C 4th row: u_i - values of the calibration velocities
C at 1st yaw angle
C 5th row: v_i - values of the anemometer output voltage
C at these 1st yaw calibration velocities
C 6th row: u_i - values of the calibration velocities
C at 2nd yaw angle
C 7th row: v_i - values of the anemometer output voltage
C at these 2nd yaw calibration velocities
C .... and so on
C write(5,*) (aco(it),it=1,mo),ex
C write(5,*) 'enter input data file name'
C read(5,*) filen
C open(2,file=filen,status='old')
C read in no. of yaw angles of calibration
C read(2,*) na
C write(5,*) na
C read in the values of those yaw angles
C read(2,*) (ate(i),i=1,na)
C write(5,*) (ate(i),i=1,na)
C read in the no. of velocity calibrations at each of these yaw angles
C read(2,*) (nu(i),i=1,na)

```

```

write(5,*) (nu(i),i=1,na)
C   read in those velocities and output voltages at each of those
C   yaw angles
do 10 i = 1,na
  read(2,*) (u(k,i),k=1,nu(i))
  read(2,*) (v(k,i),k=1,nu(i))
10  continue
C   output of the input data
do 20 j = 1,na
  write(9,15) i,ate(i),nu(i)
15  format(1x,'Data input as follows:')
1   /1x,i2,'th yaw angle value=',f7.2,
1   /1x,'no. of calibration velocities=',i2,' they are:')
  write(9,25) (u(j,i),j=1,nu(i))
25  format(1x,'U =: ',10f7.4)
  write(9,35) (v(j,i),j=1,nu(i))
35  format(1x,'V =: ',10f7.4)
20  continue
  mord = mo - 1
  if(mord.gt.3) goto 9990
  goto (100,200,300),mord
C   m = 1 - King's law
100 continue
  do 110 i = 1,na
  af = ate(i)*pi
  do 120 m = 1,nu(i)
C   effective velocity of the power of n
  uefn = (v(m,i)**2 - aco(1))/aco(2)
  if(uefn.lt.0.) uefn = 0.
C   effective velocity
  uef = uefn**(1./ex)
C   yaw function
  yawf(m,i) = uef/u(m,i)
  ak = (yawf(m,i))**2 - (sin(af))**2
  if(ak.ge.0.) yawkt(m,i) = sqrt(ak/(cos(af))**2)
  if(ak.lt.0.) yawkt(m,i) = -sqrt(-ak/(cos(af))**2)
C   negative values of yawkt represents imaginary values
120 continue
130 continue
110 continue
  goto 400
200 continue
C   m = 2 modified King's law
do 210 i = 1,na
  af = ate(i)*3.1415927/180*1
  do 220 m = 1,nu(i)
  uefn = (-aco(2) + sqrt(aco(2)**2 - 4*aco(3)*(aco(1) -
1   v(m,i)*v(m,i))))/(2*aco(3))

```

```

uef=uefn**(1./ex)
write(5,*) (aco(it),it=1,mo),ex
yawf(m,i)=uef/u(m,i)
write(5,*) u(m,i),uefn,uef,yawf(m,i)
ak=(uef/u(m,i))**2-(sin(af))**2
if(ak.ge.0.) yawkt(m,i)=sqrt(ak)/abs(cos(af))
if(ak.lt.0.) yawkt(m,i)=-sqrt(-ak)/abs(cos(af))
220 continue
210 continue
goto 400
300 continue
a=aco(4)
b=aco(3)
c=aco(2)
delta=b/(3.*a)
p=(3.*a*c-b*b)/(3.*a*a)/3.
do 310 i=1,na
af=ate(i)*3.1415927/180*1
do 310 m=1,nu(i)
d=aco(1)-(v(m,i))**2
q=(2.*b**3+27.*a*a*d-9.*a*b*c)/(27.*a**3)/2.
dpq=q*q+p*p
pq=sqrt(dpq)
pqa=(-q+pq)**(1./3.)
pqb=-(q+pq)**(1./3.)
uefn=pqa+pqb-delta
uef=uefn**(1./ex)
yawf(m,i)=uef/u(m,i)
ak=(uef/u(m,i))**2-(sin(af))**2
if(ak.ge.0.) yawkt(m,i)=sqrt(ak)/abs(cos(af))
if(ak.lt.0.) yawkt(m,i)=-sqrt(-ak)/abs(cos(af))
320 continue
310 continue
400 continue
do 410 i=1,na
num=0
sumy=0.
sumk=0.
do 420 m=1,nu(i)
C if(yawkt(m,i).le.0) goto 420
num=num+1
sumy=sumy+yawf(m,i)
sumk=sumk+yawkt(m,i)
420 continue
cmean(i)=0
cmeank(i)=0
if(num.gt.0) cmean(i)=sumy/num
if(num.gt.0) cmeank(i)=sumk/num

```

```

num=0
rmsy=0.
rmsk=0.
C
do 430 m=1,nu(i)
if(yawkt(m,i).le.0) goto 430
num=num+1
rmsy=rmsy+(cmean(i)-yawf(m,i))**2
rmsk=rmsk+(cmeank(i)-yawkt(m,i))**2
430 continue
crmsy(i)=0
crmsk(i)=0
if(num.gt.0) crmsy(i)=sqrt(rmsy/num)
if(num.gt.0) crmsk(i)=sqrt(rmsk/num)
410 continue
write(9,405) mord
405 format(/1x,'results from m=',i1
1 /1x,'negative values of kt represents imaginary values'
1 /1x,'of the yaw factor as the yaw function is less'
1 /1x,'than the sine of the yaw angle')
C
do 440 i=1,na
write(9,415) i,ate(i),nu(i)
415 format(1x,i2,'th yaw angle value=',f7.2,
1 /1x,'no. of calibration velocities=',i2,
1 /1x,'yaw function y=; yaw factor k= below:')
write(9,425) (yawf(k,i),k=1,nu(i))
425 format(1x,'y=:',10e10.2)
write(9,435) cmean(i),crmsy(i)
435 format(1x,'the mean of those yaw function values above that'
1 /1x,'are greater than the sine of yaw angle is:',f7.3
1 /1x,'their corresponding root-mean-square is ',f7.3/)
write(9,445) (yawkt(k,i),k=1,nu(i))
445 format(1x,'k=:',10f7.3)
write(9,455) cmeank(i),crmsk(i)
455 format(1x,'the mean of the yaw factor values above zero is:'
1 ,f7.3
1 /1x,'their corresponding root-mean-square is ',f7.3/)
440 continue
write(9,465) (ate(i),i=1,na)
465 format(1x,'a=',6f9.2)
C
do 450 i=1,na
write(9,475) (yawf(j,i),j=1,nu(i))
475 format(1x,6f9.3)
450 continue
goto 500
9990 continue

```

```

        write(9,505) mord
505  format(1x,'no calculation routine is available for m>3'
1    /1x,'no output is available for m=',i
1    /1x,'try another value of m no more than 3')
        return
500  continue
        norm=na+1
        nu(norm)=nx
        ate(norm)=90.
C
        do 510 i=1,nx
        u(i,norm)=unorm(i)
        v(i,norm)=vnorm(i)
510  continue
C
        do 910 i=1,norm
910  write(9,905) ate(i),(u(m,i),m=1,nu(i))
        do 920 i=1,norm
920  write(9,905) ate(i),(v(m,i),m=1,nu(i))
905  format(1x,f6.1,14f8.3)
C
        do 810 i=1,na
810  write(9,905) ate(i),(yawf(m,i),m=1,nu(i)),cmeany(i),crmsy(i)
        do 820 i=1,na
820  write(9,905) ate(i),(yawkt(m,i),m=1,nu(i)),cmeank(i),crmsk(i)
600  continue
        write(5,*) 'input a value for the yaw factor'
        read(5,*) ckt
        num=0.
        ersum=0
C
        do 520 i=1,norm
        af=ate(i)*pi
        nsub=0
        ersub=0.
C
        do 530 m=1,nu(i)
        vc(m,i)=sqrt(dif(aco,mo,cuef(u(m,i),af,ckt),0.))
        erf(m,i)=abs(vc(m,i)-v(m,i))/v(m,i)*100.
        ersum=ersum+erf(m,i)
        ersub=ersub+erf(m,i)
        nsub=nsub+1
        num=num+1
530  continue
        suber(i)=ersub/nsub
520  continue
        ersum=ersum/num
C
        root-mean-square of the errors

```

```

rms=0.
do 540 i=1,norm
nsub=0
rmsub=0.
do 550 m=1,nu(i)
rms=rms+(ersum-erf(m,i))**2
rmsub=rmsub+(suber(i)-erf(m,i))**2
nsub=nsub+1
550 continue
subrms(i)=sqrt(rmsub/nsub)
540 continue
rms=sqrt(rms/num)
write(9,515) ckt
515 format(1x,'the input yaw factor value =',f7.3/)
do 560 i=1,norm
write(9,525) i,ate(i)
525 format(1x,i2,'th yaw angle =',f7.2
1 /1x,'calculated voltages (Vc)'
1 /1x,'percentage fitting errors e(%) are'/)
write(9,535) (vc(m,i),m=1,nu(i))
535 format(1x,'Vc =',10f7.4)
write(9,545) (erf(m,i),m=1,nu(i))
545 format(1x,'e(%) =',10f7.2)
write(9,555) suber(i),subrms(i)
555 format(1x,'with a mean percentage error of',f9.4
1 /1x,'and root-mean-square of the mean error of',f9.4//)
560 continue
write(9,515) ckt
do 930 i=1,norm
write(9,905) ate(i),(vc(m,i),m=1,nu(i))
930 do 940 i=1,norm
write(9,915) ate(i),(erf(m,i),m=1,nu(i)),suber(i),subrms(i)
940 format(1x,f6.1,14f8.2)
915 write(9,565) ersum,rms
565 format(1x,'mean value of the total percentage
1 fitting errors =',f8.2
1 /1x,'with a root-mean-square value of',f8.2)
write(5,*) 'try another k_t value?(1)'
read(5,*) nret
if(nret.eq.1) goto 600
return
end

```

Program to evaluate the coefficients of two-variable non-linear polynomial

- Based on yaw calibration data
- A 3rd order polynomial was used in this study
- Used for all four sensors
- Following the program, input files and output files (voltage, velocity, curve-fitting error in percentage at each point, corrected voltage, coefficients of two-variable non-linear polynomial) have been attached

```

C   THIS PROGRAM CURVE FITS DATA BASED ON
C   TWO-VARIABLE NON-LINEAR EQUATION AS DESCRIBED
C   IN THE REPORT. THIS PROGRAM WAS USED TO CURVE FIT
C   YAW CALIBRATION DATA. A THIRD ORDER POLYNOMIAL WAS
C   USED IN THIS WORK.
C
C   NX - NUMBER OF CALIBRATION ANGLES SHOULD BE SET INITIALLY
C   BEFORE COMPILING THE PROGRAM
C
C   MO - ORDER OF POLYNOMIAL + 1 SHOULD ALSO BE SET INITIALLY
C   IMPLICIT REAL*8 (A-H,O-Z)
C   PARAMETER (NX=8,MO=4,API=3.1415926536/180.)
C   PARAMETER (MS=MO*(MO+1)/2)
C   PARAMETER (MT=MS+45)
C   DIMENSION X(NX),Y(NX,30),Z(NX,30),A(MS,MS),C(MT)
C   DIMENSION NY(30),ERXYZ(30,NX),YT(NX,30),ZT(NX,30)
C   DIMENSION D3XYZ(30,NX),D3CON(NX,30),g(30,NX),H(30,NX)
C   DATA Y,Z,G,H/960*0./
C   EXTERNAL ZXYFIT
C   OPEN(2,FILE='?yaw.DAT',STATUS='OLD')
C   OPEN(3,FILE='?YAWO.DAT',STATUS='NEW')
C   OPEN(4,FILE='?YAWU.DAT',STATUS='NEW')
C   OPEN(7,FILE='?YAWV.DAT',STATUS='NEW')
C   OPEN(8,FILE='?YAWVC.DAT',STATUS='NEW')
C   YAWO.DAT- ASSORTED OUTPUT
C   YAWU.DAT- CALIBRATION VELOCITY
C   YAWV.DAT- CALIBRATION VOLTAGE
C   YAWVC.DAT- FITTED VOLTAGE
C   do 998 iret=1,1
C   READ(2,*) (X(I),I=1,NX)
C   READ(2,*) (NY(I),I=1,NX)
C   DO 10 I=1,NX
C   READ(2,*) (Y(I,J),J=1,NY(I))
10  READ(2,*) (Z(I,J),J=1,NY(I))
C   do 9 i=1,nx
9   x(i)=x(i)*api
C   call npoly(ex,y,z,yt,zt,nx,ny,x,mo,ms,a,c,
C   1 tse,tseod,erxyz)
C   call trans(ex,y,i,nx,ny,yt,zt)
C   CALL ZXYFIT(X,NX,YT,NY,ZT,A,C,MO,MS,TSE,ERXYZ)
60  FORMAT(1X,'a*s=' ,5E15.7)
C   write(3,60) tse,ex
C   write(3,60) (c(i),i=1,ms)
C   calculation of the sum of the squared errors in equation (10)
C   TSEOD=0.
C   DO 100 I=1,NX
C   DO 200 J=1,NY(I)
C   yt(i,j)=(j*0.15)**ex

```

```

SUBT=0.
NUVS=0
DO 110 IU=1,MO
JU=IU-1
DO 210 IV=1,IU
JV=IV-1
XPART=1
IF(ABS(X(I))+JV.GT.0) XPART=X(I)**JV
YPART=1
IF(ABS(YT(I,J))+ABS(JU-JV).GT.0) YPART=YT(I,J)**(JU-JV)
NUVS=NUVS+1
SUBT=SUBT+C(NUVS)*XPART*YPART
210 CONTINUE
110 CONTINUE
TSEOD=(Z(I,J)-SQRT(SUBT))**2+TSEOD
ERXYZ(I,J)=ABS(Z(I,J)-SQRT(SUBT))/Z(I,J)*100.
d3xyz(j,i)=sqrt(subt)
200 CONTINUE
100 CONTINUE
WRITE(3,60) TSEOD,EX
WRITE(3,51) ((ERXYZ(I,J),J=1,NX),I=1,14)
51 FORMAT(1X,7F7.4)
DO 301 I=1,NX
DO 301 J=1,14
H(J,I)=Z(I,J)
301 G(J,I)=Y(I,J)
WRITE(4,71) ((G(I,J),J=1,NX),I=1,14)
WRITE(7,71) ((H(I,J),J=1,NX),I=1,14)
WRITE(8,71) ((D3XYZ(I,J),J=1,NX),I=1,14)
71 FORMAT(1X,7F7.4)
998 continue
STOP
END
C
subroutine npoly(ex,u,v,yt,zt,nx,ny,x,mo,ms,coef,cn,tse,tseod,erxyz)
implicit real*8 (a-h,o-z)
dimension u(nx,30),v(nx,30),yt(nx,30),zt(nx,30),x(nx)
dimension ny(30),erxyz(nx,30),coef(ms,ms),a(45),cn(ms)
ex=0.3
ex0=ex
tc=ex
call fabn(tc,u,v,yt,zt,nx,ny,x,mo,ms,coef,cn,tse0,tseod0,erxyz)
do 20 i=1,30
tc=ex0+0.01*i
call fabn(tc,u,v,yt,zt,nx,ny,x,mo,ms,coef,a,tse,tseod,erxyz)
if(tse.ge.tse0) goto 20
ex=tc
tse0=tse

```

```

do 25 it=1,ms
25  cn(it)=a(it)
20  continue
   cc=ex
   do 30 i=1,10
   tc=cc+0.001*i
   call fabn(tc,u,v,yt,zt,nx,ny,x,mo,ms,coef,a,tse,tseod,erxyz)
   if(tse.ge.tse0) goto 40
   ex=tc
   tse0=tse
   do 45 it=1,ms
45  cn(it)=a(it)
40  continue
   tc=cc-0.001*i
   call fabn(tc,u,v,yt,zt,nx,ny,x,mo,ms,coef,a,tse,tseod,erxyz)
   if(tse.ge.tse0) goto 30
   ex=tc
   tse0=tse
   do 35 it=1,ms
35  cn(it)=a(it)
30  continue
   cc=ex
   do 50 i=1,10
   tc=cc+0.0001*i
   call fabn(tc,u,v,yt,zt,nx,ny,x,mo,ms,coef,a,tse,tseod,erxyz)
   if(tse.ge.tse0) goto 60
   ex=tc
   tse0=tse
   do 55 it=1,ms
55  cn(it)=a(it)
60  continue
   tc=cc-0.0001*i
   call fabn(tc,u,v,yt,zt,nx,ny,x,mo,ms,coef,a,tse,tseod,erxyz)
   if(tse.ge.tse0) goto 50
   :x=tc
   tse0=tse
   do 65 it=1,ms
65  cn(it)=a(it)
50  continue
   return
   end

```

```

C
subroutine fabn(ex,u,v,yt,zt,nx,ny,x,mo,ms,a,c,tse,
1 tseod,erxyz)
implicit real*8 (a-h,o-z)
dimension u(nx,30),v(nx,30),yt(nx,30),zt(nx,30),x(nx)
dimension ny(30),a(ms,ms),b(45),c(ms),erxyz(nx,30)
call trans(ex,u,v,nx,ny,yt,zt)

```

```

CALL ZXYFIT(X,NX, YT,NY, ZT,A,C,MO,MS,TSE,ERXYZ)
tseed=0.
return
end
subroutine trans(ex,u,v,nx,ny,yt,zt)
implicit real*8 (a-h,o-z)
dimension u(nx,30),v(nx,30),yt(nx,30),zt(nx,30),ny(30)
do 10 i=1,nx
do 10 j=1,ny(i)
yt(i,j)=u(i,j)**ex
zt(i,j)=v(i,j)**2
10 continue
return
end
C This subroutine curve fits a two-variable polynomial to a set
C of (x,y,z) data by means of a least squares regression
SUBROUTINE ZXYFIT(X,NX,Y,NY,Z,A,C,MO,MS,TSE,ERXYZ)
IMPLICIT REAL*8 (A-H,O-Z)
DIMENSION X(NX),Y(NX,30),Z(NX,30),A(MS,MS),B(45),C(MS)
DIMENSION NY(NX),ERXYZ(NX,30)
C F(x,y)=Sum(i=0;n)Sum c_ij x^j y^i-j (j=0;i)
C (n=2)=c_00 +c_10y+c_11x+c_20y^2+c_21xy+c_22x^2
C NX: data points - x
C NY: data points - y
C MO-1=n: order of the polynomial
C MS=SUM i (i=1;MO)=MO(MO+1)/2: the number of coefficients c_ij
C MO<=9 is set in the program (i.e. B(45))
NS=0
DO 555 I=1,MO
NS=NS+1
555 CONTINUE
IF(NS.EQ.MS) GOTO 15
WRITE(5,25) MO,MS
25 FORMAT(1X,'M AND MS ARE INCOMPATIBLE'
1 /1X,'M+1=',15
1 /1X,'Ms=',16
1 /1X,'DOUBLE CHECK PROGRAM INPUT AND START AGAIN!'/))
RETURN
15 CONTINUE
NUVS=0
DO 10 IU=1,MO
JU=IU-1
DO 20 IV=1,IU
JV=IV-1
NUVS=NUVS+1
SZ=0.0
DO 110 I=1,NX
DO 120 J=1,NY(I)

```

```

XPART=1
IF(ABS(X(I))+JV.GT.0) XPART=X(I)**JV
YPART=1
IF(ABS(Y(I,J))+ABS(JU-JV).GT.0) YPART=Y(I,J)**(JU-JV)
SZ=SZ+Z(I,J)*XPART*YPART
120 CONTINUE
110 CONTINUE
B(NUVS)=SZ
NMNS=0
DO 210 N=1,MO
JN=N-1
DO 220 M=1,N
JM=M-1
NMNS=NMNS+1
SXY=0.0
DO 215 I=1,NX
DO 225 J=1,NY(I)
XPART=1
IF(ABS(X(I))+JV+JM.GT.0) XPART=X(I)**(JV+JM)
YPART=1
IF(ABS(Y(I,J))+ABS(JN+JU-JM-JV).GT.0)
YPART=Y(I,J)**(JN+JU-JM-JV)
SXY=SXY+XPART*YPART
225 CONTINUE
215 CONTINUE
A(NUVS,NMNS)=SXY
220 CONTINUE
210 CONTINUE
20 CONTINUE
10 CONTINUE
C CALL DLSARG(NUVS,A,NUVS,B,1,C)
SUM OF THE SQUARED ERRORS
TSE=0.
DO 300 I=1,NX
DO 400 J=1,NY(I)
SUBT=0.
NUVS=0
DO 310 IU=1,MO
JU=IU-1
DO 410 IV=1,IU
JV=IV-1
NUVS=NUVS+1
XPART=1
IF(ABS(X(I))+JV.GT.0) XPART=X(I)**JV
YPART=1
IF(ABS(Y(I,J))+ABS(JU-JV).GT.0) YPART=Y(I,J)**(JU-JV)
SUBT=SUBT+C(NUVS)*XPART*YPART
410 CONTINUE

```

```
310 CONTINUE
      TSE=(Z(I,J)-SUBT)**2+TSE
      ERXYZ(I,J)=ABS(Z(I,J)-SUBT)/ABS(Z(I,J))
      write(3,34) x(i),y(i,j),sqrt(z(i,j)),
1             sqrt(subt),sqrt(erxyz(i,j))*100
400 CONTINUE
300 CONTINUE
      write(3,34) (c(i),i=1,10)
      RETURN
34  format(1x,5c12.4)
      END
```

YAW CALIBRATION FOR SENSOR ONE

INPUT FILE 1YAW.DAT

YAW ANGLES

90. 80. 70. 60. 50. 30. 20. 10. 0.

NUMBER OF CALIBRATION SPEEDS AT EACH YAW ANGLE

8 9 9 9 9 9 9 9

VELOCITY AND VOLTAGE FOR 1ST YAW ANGLE

0.0000 0.1219 0.2475 0.5000 0.7516 1.2551 1.7595 2.2620
3.5939 6.5749 7.0887 7.8063 8.2105 8.6842 8.9490 9.1592

VELOCITY AND VOLTAGE FOR 2ND YAW ANGLE

0.0000 0.1229 0.2476 0.5007 0.7528 1.1053 1.4556 1.8087 2.2620
3.7514 6.5025 7.0725 7.7232 8.0513 8.4184 8.6474 8.7823 8.9131

AND SO ON

0.0000 0.1221 0.2475 0.4993 0.7514 1.1040 1.4570 1.8083 2.2618
3.9790 6.4170 6.9841 7.6199 7.9688 8.3086 8.5236 8.6921 8.8376

0.0000 0.1222 0.2475 0.4996 0.7512 1.1045 1.4562 1.8078 2.2626
3.6666 6.2369 6.8323 7.4417 7.8078 8.1379 8.3583 8.4992 8.6951

0.0000 0.1224 0.2473 0.4995 0.7513 1.1029 1.4562 1.8070 2.2599
3.5371 6.0439 6.6051 7.2915 7.6395 7.9967 8.1972 8.3392 8.5250

0.0000 0.1218 0.2473 0.4993 0.7512 1.1042 1.4548 1.8079 2.2598
3.6347 5.8492 6.4193 7.0087 7.3719 7.7867 8.0225 8.2326 8.4049

0.0000 0.1216 0.2477 0.4997 0.7503 1.1036 1.4553 1.8081 2.2612
3.5834 5.6586 6.2365 6.8100 7.1474 7.5467 7.8462 8.0476 8.2627

0.0000 0.1228 0.2473 0.4998 0.7516 1.1035 1.4557 1.8087 2.2610
3.6721 5.4483 5.9601 6.6105 6.9206 7.2408 7.4854 7.6756 7.9242

0.0000 0.1219 0.2477 0.4994 0.7510 1.1041 1.4559 1.8087 2.2622
3.6774 5.2638 5.7768 6.4423 6.6945 7.0034 7.2990 7.5517 7.9066

OUTPUT FILE (1YAWO.DAT)

EXPONENT, n = 0.4382000E+00

COEFFICIENTS OF POLYNOMIAL

a*s= 0.1220425E+02 0.4327622E+02 0.6001274E+01 -0.8467405E+01 0.2723703E+02

a*s= -0.6654442E+01 0.1469114E+01 -0.1230175E+02 -0.6318249E+00 0.2228492E+01

PERCENTAGE ERROR AT EACH POINT - EACH VALUE CORRESPONDS TO RESPECTIVE COMPONENTS IN OUTPUT FILES 1YAWU.DAT, 1YAWV.DAT AND 1YAWVC.DAT.

3.5484 1.4185 7.0884 1.1337 5.2328 2.3603 2.8498
1.5829 5.0019 0.0941 0.7616 1.2853 0.1723 1.2074
0.2446 0.8977 1.5601 0.8239 1.4691 0.2199 0.8043
0.4423 1.0311 0.5032 0.3061 0.9538 0.0802 0.5966
0.1929 0.7085 0.1792 0.0623 0.4994 0.2813 0.4578
1.6930 0.2743 0.4434 0.3210 0.0737 0.2397 0.4529
0.0548 0.2865 0.0213 0.1013 0.1079 0.2595 0.1340
0.1075 1.2179 0.5078 0.8173 0.8026 0.3168 0.0426
0.0595 0.3248 0.6344 0.9485 0.9617 1.1384 0.5492
1.0419 0.2986 0.1022 0.6976 1.0895 1.0571 0.8533
1.4760 0.2214 0.0975 0.3749 0.0434 0.3093 0.9463
0.6919 0.8265 1.1925 1.1603

OUTPUT FILE (1YAWU.DAT)

THIS IS THE SEQUENCE IN WHICH VELOCITY IS READ AND OTHER OUTPUT FILES SHOULD BE READ ACCORDINGLY.

0.0000 0.0000 0.0000 0.0000 0.0000 0.0000 0.0000 0.0000
0.0000 0.0000 0.1219 0.1229 0.1221 0.1222 0.1224
0.1218 0.1216 0.1228 0.1219 0.2475 0.2476 0.2475
0.2475 0.2473 0.2473 0.2477 0.2473 0.2477 0.5000
0.5007 0.4993 0.4996 0.4995 0.4993 0.4997 0.4998
0.4994 0.7516 0.7528 0.7514 0.7512 0.7513 0.7512
0.7503 0.7516 0.7510 1.2551 1.1053 1.1040 1.1045
1.1029 1.1042 1.1036 1.1035 1.1041 1.7595 1.4556
1.4570 1.4562 1.4562 1.4548 1.4553 1.4557 1.4559
2.2620 1.8087 1.8083 1.8078 1.8070 1.8079 1.8081
1.8087 1.8087 0.0000 2.2620 2.2618 2.2626 2.2599
2.2598 2.2612 2.2610 2.2622

OUTPUT FILE (1YAWV.DAT)

THE VOLTAGES ARE READ IN CONJUNCTION WITH VELOCITY AS ABOVE

3.5939 3.7514 3.9790 3.6666 3.5371 3.6347 3.5834
3.6721 3.6774 6.5749 6.5025 6.4170 6.2369 6.0439
5.8492 5.6586 5.4483 5.2638 7.0887 7.0725 6.9841
6.8323 6.6051 6.4193 6.2365 5.9601 5.7768 7.8063
7.7232 7.6199 7.4417 7.2915 7.0087 6.8100 6.6105
6.4423 8.2105 8.0513 7.9688 7.8078 7.6395 7.3719
7.1474 6.9206 6.6945 6.6842 8.4184 8.3086 8.1379
7.9967 7.7867 7.5467 7.2408 7.0034 8.9490 8.6474
8.5236 8.3583 8.1972 8.0225 7.8462 7.4854 7.2990
9.1592 8.7823 8.6921 8.4992 8.3392 8.2326 8.0476
7.6756 7.5517 0.0000 8.9131 8.8376 8.6951 8.5250
8.4049 8.2627 7.9242 7.9066

OUTPUT FILE (1YAWVC.DAT)

THESE ARE THE CORRECTED VOLTAGES WHICH CORRESPOND TO INPUT VOLTAGES AS ABOVE AND PERCENTAGE ERRORS ARE CALCULATED BASED ON THESE VOLTAGES.

3.7214 3.6982 3.6970 3.7082 3.7222 3.7205 3.6855
3.6140 3.4935 6.5687 6.4530 6.3345 6.2262 6.1169
5.8635 5.7094 5.5333 5.3072 7.1928 7.0569 6.9279
6.8021 6.6732 6.3870 6.2174 6.0169 5.7814 7.8529
7.7083 7.5659 7.4284 7.2870 6.9737 6.7908 6.5802
6.3332 8.2330 8.0870 7.9432 7.8020 7.6578 7.3385
7.1513 6.9404 6.6931 8.6754 8.4275 8.2870 8.1488
8.0053 7.6919 7.5084 7.3000 7.0596 8.9207 8.6511
8.5185 8.3854 8.2492 7.9464 7.7707 7.5706 7.3391
9.0638 8.8085 8.6832 8.5585 8.4301 8.1456 7.9789
7.7889 7.5684 0.0000 8.9465 8.8338 8.7220 8.6057
8.3467 8.1944 8.0187 7.8149

YAW CALIBRATION FOR SENSOR TWO

INPUT FILE 2YAW.DAT

YAW ANGLES

90.,80.,70.,60.,50.

NUMBER OF CALIBRATION SPEEDS AT EACH YAW ANGLE

7,7,7,7

VELOCITY AND VOLTAGE FOR 1ST YAW ANGLE

0.00000 0.1216859 0.2476904 0.4991713 0.7507274 1.0027877 1.2544831
3.59942 6.5454104 7.1285299 7.8289808 8.3037584 8.5714576 8.8044153

VELOCITY AND VOLTAGE FOR 2ND YAW ANGLE

0.00000 0.1208484 0.2472025 0.4998467 0.7513150 1.0030194 1.2540653
3.58775 6.5282299 7.1064190 7.8204380 8.2324315 8.5227296 8.7360453

AND SO ON

0.00000 0.1209240 0.2476937 0.4988643 0.7518545 1.0023250 1.2544291
3.92806 6.4652101 7.0282578 7.6896044 8.0965038 8.4099796 8.6142292

0.00000 0.1217322 0.2478858 0.4988679 0.7512782 1.0011019 1.2535622
3.92806 6.3435063 6.8830784 7.5361953 7.9341163 8.1975160 8.4189789

0.00000 0.1215208 0.2476971 0.4990944 0.7505847 1.0035379 1.2552515
3.92806 6.0737267 6.6392206 7.2914238 7.7144235 7.9851367 8.2050367

OUTPUT FILE (2YAWO.DAT)

EXPONENT, n = 0.2983000E+00

COEFFICIENTS OF POLYNOMIAL

a*s = 0.1002288E+01 -0.1352662E+02 0.3280068E+02 0.5978110E+02 0.4470655E+02
a*s = -0.2184441E+02 -0.2391659E+02 -0.8845916E+01 -0.7127153E+01 0.3561689E+01

PERCENTAGE ERROR AT EACH POINT - EACH VALUE CORRESPONDS TO RESPECTIVE COMPONENTS IN OUTPUT FILES 2YAWU.DAT, 2YAWV.DAT AND 2YAWVC.DAT.

2.0470 3.9504 1.5161 0.1828 0.2333 0.1366 0.2819
0.4092 0.5152 0.4642 0.4966 0.2303 0.0943 0.0315
0.3290 0.3266 0.2358 0.0775 0.0699 0.0445 0.3249
0.1848 0.1255 0.0037 0.3113 0.0627 0.1112 0.1495
0.2825 0.1136 0.0012 0.0247 0.0780 0.2745 0.1385

OUTPUT FILE (2YAWU.DAT)

THIS IS THE SEQUENCE IN WHICH VELOCITY IS READ AND OTHER OUTPUT FILES SHOULD BE READ ACCORDINGLY.

0.0000 0.0000 0.0000 0.0000 0.0000 0.1217 0.1208
0.1209 0.1217 0.1215 0.2477 0.2472 0.2477 0.2479
0.2477 0.4992 0.4998 0.4989 0.4989 0.4991 0.7507
0.7513 0.7519 0.7513 0.7506 1.0028 1.0030 1.0023
1.0011 1.0035 1.2545 1.2541 1.2544 1.2536 1.2553

OUTPUT FILE (2YAWV.DAT)

THE VOLTAGES ARE READ IN CONJUNCTION WITH VELOCITY IN THE SAME MANNER AS OUTPUT FILE (2YAWU.DAT)

3.5994 3.5878 3.9281 3.9281 3.9281 6.5454 6.5282
6.4652 6.3435 6.0737 7.1285 7.1064 7.0283 6.8831
6.6392 7.8290 7.8204 7.6896 7.5362 7.2914 8.3038
8.2324 8.0965 7.9341 7.7144 8.5715 8.5227 8.4100
8.1975 7.9851 8.8044 8.7360 8.6142 8.4190 8.2050

OUTPUT FILE (2YAWVC.DAT)

THESE ARE THE CORRECTED VOLTAGES WHICH CORRESPOND TO INPUT VOLTAGES AS IN OUTPUT FILE (1YAWV.DAT) AND PERCENTAGE ERROR AT EACH POINT IS BASED ON THESE VOLTAGES AND THE CORRESPONDING VOLTAGE IN OUTPUT FILE (2YAWV.DAT)

3.5257 3.7295 3.8685 3.9352 3.9189 6.5365 6.5098
6.4388 6.3108 6.1019 7.1639 7.1228 7.0349 6.8852
6.6611 7.8546 7.8020 7.6956 7.5309 7.2947 8.2768
8.2177 8.1067 7.9344 7.6904 8.5768 8.5132 8.3974
8.2207 7.9761 8.8043 8.7382 8.6209 8.4421 8.1937

YAW CALIBRATION FOR SENSOR THREE

INPUT FILE 3YAW.DAT

YAW ANGLES

80.,90.,70.,60.,50.,30.,20.,10.,0.

NUMBER OF CALIBRATION SPEEDS AT EACH YAW ANGLE

10,10,10,10,10,8,8,8

VELOCITY AND VOLTAGE FOR 1ST YAW ANGLE

0.0000 0.1215 0.2472 0.4993 0.7511 1.0033 1.2551 1.5068 1.8079 2.2607
3.4799 5.6856 6.2099 6.8136 7.1516 7.4376 7.6283 7.7673 7.9294 8.0615

VELOCITY AND VOLTAGE FOR 2ND YAW ANGLE

0.0000 0.1215 0.2472 0.4991 0.7507 1.0038 1.2548 1.5059 1.8081 2.2627
3.4879 5.7964 6.3280 6.9313 7.2891 7.5831 7.7680 7.9224 8.0799 8.2179

AND SO ON

0.0000 0.1217 0.2476 0.4997 0.7512 1.0030 1.2546 1.5064 1.8083 2.2609
3.4933 5.6245 6.1707 6.7133 7.1248 7.4648 7.5915 7.6779 7.7516 7.8683

0.0000 0.1217 0.2477 0.4993 0.7505 1.0031 1.2548 1.5064 1.8079 2.2610
3.7213 5.5963 6.1089 6.6355 6.9050 7.2676 7.4630 7.5966 7.7034 7.8604

0.0000 0.1220 0.2480 0.4990 0.7509 1.0030 1.2546 1.5060 1.8072 2.2614
3.3328 5.3524 5.8867 6.4072 6.6477 6.9454 7.1742 7.2598 7.3528 7.4664

0.0000 0.1218 0.2469 0.4991 0.7498 1.2541 1.8083 2.2601
3.5792 5.2206 5.6935 6.2998 6.6165 7.0401 7.2813 7.4174

0.0000 0.1215 0.2472 0.4996 0.7501 1.2540 1.8079 2.2596
3.3185 5.0833 5.5618 6.0613 6.4006 6.8688 7.2042 7.3204

0.0000 0.1212 0.2478 0.5000 0.7499 1.2545 1.8080 2.2604
3.4428 4.9572 5.4337 5.8917 6.1969 6.7128 7.0539 7.2168

0.0000 0.1201 0.2471 0.4988 0.7510 1.2540 1.8081 2.2609
3.4479 4.7683 5.1626 5.5546 5.7718 6.2730 6.6828 6.8915

OUTPUT FILE (3YAWO.DAT)

EXPONENT, a = 0.4503000E+00

COEFFICIENTS OF POLYNOMIAL

a*s= 0.1079219E+02 0.3037168E+02 0.8068669E+01 -0.1703726E+01
0.1852357E+02
a*s= -0.9580333E+01 -0.1029914E+01 -0.8288538E+01 0.7931897E+00
0.3164674E+01

PERCENTAGE ERROR AT EACH POINT - EACH VALUE CORRESPONDS TO RESPECTIVE COMPONENTS IN OUTPUT FILES 3YAWU.DAT, 3YAWV.DAT AND 3YAWVC.DAT.

0.4733 0.2962 0.3366 5.4876 6.6785 0.1328 6.8633
0.3056 4.7204 0.0219 0.0080 0.5698 1.5303 1.5052
0.4286 0.5472 0.3604 1.2420 0.3889 0.5590 0.7617
1.4124 0.6407 0.0282 0.2185 1.2109 0.5947 0.3522
0.7198 0.0404 0.6596 1.0637 1.2872 0.0072 0.3830
1.3364 0.6675 0.8208 0.8384 0.4953 2.5474 1.0399
0.2318 0.0837 3.1910 0.1755 0.2707 2.0293 1.1279
1.6564 0.9273 0.7894 1.2906 1.9939 0.1029 0.2691
1.2280 1.2427 0.9860 0.1550 1.1935 1.6087 0.6589
0.1354 0.0884 0.4800 1.0868 1.7944 0.2673 0.3495
1.2281 0.5255 0.2897 0.2934 0.2694 0.7184 2.3706
0.0000 0.0000 0.0000 0.0000 0.2638 0.3991 0.5527
0.8500 2.8558 0.0000 0.0000 0.0000 0.0000 0.0002

OUTPUT FILE (3YAWU.DAT)

THIS IS THE SEQUENCE IN WHICH VELOCITY IS READ AND OTHER OUTPUT FILES SHOULD BE READ ACCORDINGLY.

0.0000 0.0000 0.0000 0.0000 0.0000 0.0000 0.0000
0.0000 0.0000 0.1215 0.1215 0.1217 0.1217 0.1220
0.1218 0.1215 0.1212 0.1201 0.2472 0.2472 0.2476
0.2477 0.2480 0.2469 0.2472 0.2478 0.2471 0.4993
0.4991 0.4997 0.4993 0.4990 0.4991 0.4996 0.5000
0.4988 0.7511 0.7507 0.7512 0.7505 0.7509 0.7498
0.7501 0.7499 0.7510 1.0033 1.0038 1.0030 1.0031
1.0030 1.2541 1.2540 1.2545 1.2540 1.2551 1.2548
1.2546 1.2548 1.2546 1.8083 1.8079 1.8080 1.8081
1.5068 1.5059 1.5064 1.5064 1.5060 2.2601 2.2596
2.2604 2.2609 1.8079 1.8081 1.8083 1.8079 1.8072
0.0000 0.0000 0.0000 0.0000 2.2607 2.2627 2.2609
2.2610 2.2614 0.0000 0.0000 0.0000 0.0000 0.0000

OUTPUT FILE (3YAWV.DAT)

THE VOLTAGES ARE READ IN CONJUNCTION WITH VELOCITY IN THE SAME MANNER AS OUTPUT FILE (3YAWU.DAT)

3.4799 3.4879 3.4933 3.7213 3.3328 3.5792 3.3185
3.4428 3.4479 5.6856 5.7964 5.6245 5.5963 5.3524
5.2206 5.0833 4.9572 4.7683 6.2099 6.3280 6.1707
6.1089 5.8867 5.6935 5.5618 5.4337 5.1626 6.8136
6.9313 6.7133 6.6355 6.4072 6.2998 6.0613 5.8917
5.5546 7.1516 7.2891 7.1248 6.9050 6.6477 6.6165
6.4006 6.1969 5.7718 7.4376 7.5831 7.4648 7.2676
6.9454 7.0401 6.8688 6.7128 6.2730 7.6283 7.7680
7.5915 7.4630 7.1742 7.2813 7.2042 7.0539 6.6828
7.7673 7.9224 7.6779 7.5966 7.2598 7.4174 7.3204
7.2168 6.8915 7.9294 8.0799 7.7516 7.7034 7.3528
0.0000 0.0000 0.0000 0.0000 8.0615 8.2179 7.8683
7.8604 7.4664 0.0000 0.0000 0.0000 0.0000 0.0000

OUTPUT FILE (3YAWVC.DAT)

THESE ARE THE CORRECTED VOLTAGES WHICH CORRESPOND TO INPUT VOLTAGES AS IN OUTPUT FILE (3YAWV.DAT) AND PERCENTAGE ERROR AT EACH POINT IS BASED ON THESE VOLTAGES AND THE CORRESPONDING VOLTAGE IN OUTPUT FILE (3YAWV.DAT)

3.4634 3.4776 3.4815 3.5171 3.5554 3.5840 3.5463
3.4533 3.2851 5.6844 5.7969 5.5925 5.5107 5.4330
5.2430 5.1111 4.9393 4.7091 6.2340 6.3634 6.1237
6.0226 5.9244 5.6951 5.5496 5.3679 5.1319 6.8376
6.9812 6.7106 6.5917 6.4754 6.2187 6.0609 5.8691
5.6288 7.1993 7.3489 7.0651 6.9392 6.8170 6.5477
6.3858 6.1917 5.9560 7.4507 7.6036 7.3133 7.1856
7.0604 6.9748 6.8146 6.6262 6.3981 7.6361 7.7889
7.4983 7.3703 7.2449 7.2700 7.1182 6.9404 6.7268
7.7778 7.9294 7.6410 7.5140 7.3901 7.4372 7.2948
7.1282 6.9277 7.9064 8.0562 7.7725 7.6481 7.5271
0.0000 0.0000 0.0000 0.0000 8.0402 8.1851 7.9118
7.7936 7.6796 0.0000 0.0000 0.0000 0.0000 0.0000

YAW CALIBRATION FOR SENSOR FIVE

INPUT FILE 5YAW.DAT

YAW ANGLES

90., 80., 70., 60., 30., 20., 10., 0.

NUMBER OF CALIBRATION SPEEDS AT EACH YAW ANGLE

7,7,7,7,7,7,7

VELOCITY AND VOLTAGE FOR 1ST YAW ANGLE

0.0000 0.1211 0.2481 0.4999 0.7512 1.0053 1.2556
3.8943 6.9126 7.5380 8.2600 8.7035 9.0153 9.2221

VELOCITY AND VOLTAGE FOR 2ND YAW ANGLE

0.0000 0.1213 0.2478 0.4988 0.7502 1.0027 1.2556
3.9695 6.8795 7.4863 8.2252 8.6520 8.9250 9.1174

AND SO ON

0.0000 0.1215 0.2486 0.4999 0.7508 1.0033 1.2554
3.9235 6.7760 7.3476 8.0775 8.4841 8.7491 8.9455

0.0000 0.1222 0.2465 0.5002 0.7505 1.0035 1.2554
3.9048 6.6113 7.1853 7.8803 8.2826 8.5293 8.7019

0.0000 0.1220 0.2472 0.4991 0.7505 1.0027 1.2537
3.7920 6.1178 6.6837 7.2823 7.6601 7.9633 8.1754

0.0000 0.1218 0.2476 0.4999 0.7515 1.0039 1.2554
3.9872 5.9599 6.5335 7.1471 7.4954 7.7659 7.8692

0.0000 0.1221 0.2478 0.4999 0.7510 1.0039 1.2557
3.9007 5.7914 6.3539 6.8807 7.1855 7.4436 7.6307

0.0000 0.1216 0.2483 0.4993 0.7523 1.0039 1.2554
3.8899 5.5822 6.1106 6.4814 6.8960 7.0796 7.2655

OUTPUT FILE (SYAWO.DAT)

EXPONENT, $n = 0.3732000E+00$

COEFFICIENTS OF POLYNOMIAL

$a^*s = 0.1522256E+02 \ 0.2820532E+02 \ -0.3352675E+00 \ 0.2203975E+02 \ 0.3390235E+02$
 $a^*s = 0.6292516E+00 \ -0.1480970E+02 \ -0.7243170E+01 \ -0.4671103E+01 \ -0.2189680E+00$

PERCENTAGE ERROR AT EACH POINT - EACH VALUE CORRESPONDS TO RESPECTIVE COMPONENTS IN OUTPUT FILES SYAWU.DAT, SYAWV.DAT AND SYAWVC.DAT.

0.7695 1.1868 0.1332 0.2051 2.7740 2.3064 0.1099
0.3010 0.2451 0.6722 0.7591 0.0700 0.7008 0.4126
0.0916 0.1326 0.7045 0.0755 0.1705 0.4011 0.4103
0.3407 0.9631 0.8988 0.5132 0.5358 0.3664 0.2008
0.6449 0.6108 0.3819 1.5331 0.2387 0.6063 0.2952
0.1971 0.5420 0.4643 0.1130 0.0881 0.0016 0.4229
0.0690 0.5809 0.0596 0.7613 0.2114 0.5746 0.0125
0.2347 0.0379 0.9118 0.3851 0.1876 0.4626 0.1441

OUTPUT FILE (SYAWU.DAT)

THIS IS THE SEQUENCE IN WHICH VELOCITY IS READ AND OTHER OUTPUT FILES SHOULD BE READ ACCORDINGLY.

0.0000 0.0000 0.0000 0.0000 0.0000 0.0000 0.0000
0.0000 0.1211 0.1213 0.1215 0.1222 0.1220 0.1218
0.1221 0.1216 0.2481 0.2478 0.2486 0.2465 0.2472
0.2476 0.2478 0.2483 0.4999 0.4988 0.4999 0.5002
0.4991 0.4999 0.4999 0.4993 0.7512 0.7502 0.7508
0.7505 0.7505 0.7515 0.7510 0.7523 1.0053 1.0027
1.0033 1.0035 1.0027 1.0039 1.0039 1.0039 1.2561
1.2556 1.2554 1.2554 1.2537 1.2554 1.2557 1.2554

OUTPUT FILE (SYAWV.DAT)

THE VOLTAGES ARE READ IN CONJUNCTION WITH VELOCITY IN THE SAME MANNER AS OUTPUT FILE (SYAWU.DAT)

3.8943 3.9695 3.9235 3.9048 3.7920 3.9872 3.9007
3.8899 6.9126 6.8795 6.7760 6.6113 6.1178 5.9599
5.7914 5.5822 7.5380 7.4863 7.3476 7.1853 6.6837
6.5335 6.3539 6.1106 8.2600 8.2252 8.0775 7.8803
7.2823 7.1471 6.8807 6.4814 8.7035 8.6520 8.4841
8.2826 7.6601 7.4954 7.1855 6.8960 9.0153 8.9250
8.7491 8.5293 7.9633 7.7659 7.4436 7.0796 9.2221
9.1174 8.9455 8.7019 8.1754 7.8692 7.6307 7.2655

OUTPUT FILE (SYAWVC.DAT)

THESE ARE CORRECTED VOLTAGES WHICH CORRESPOND TO INPUT VOLTAGES AS IN OUTPUT FILE (SYAWV.DAT) AND PERCENTAGE ERROR AT EACH POINT IS BASED ON THESE VOLTAGES AND THE CORRESPONDING VOLTAGE IN OUTPUT FILE (SYAWV.DAT)

3.9243 3.9224 3.9183 3.9128 3.8972 3.8952 3.8964
3.9016 6.9295 6.8333 6.7246 6.6067 6.1607 5.9845
5.7967 5.5896 7.5911 7.4806 7.3601 7.2141 6.7111
6.5112 6.2927 6.0557 8.3024 8.1811 8.0479 7.8961
7.3293 7.1034 6.8544 6.5808 8.7243 8.5995 8.4591
8.2989 7.7016 7.4606 7.1936 6.9021 9.0154 8.8873
8.7431 8.5788 7.9586 7.7068 7.4279 7.1203 9.2233
9.0960 8.9489 8.7812 8.1439 7.8840 7.5954 7.2760

Program to iterate values of velocity and yaw angle for a given voltage

- The three sets of coefficients (one set each for the sensors) based on the two-variable non-linear polynomial was used in the program.
- Used to analyze CTA wake survey data
- Program converged for known value of voltage, velocity and yaw angle (based on the yaw calibration model - checked for all 4 sensors)
- Routine - Coefficients established for the three sensors based on the two-variable non-linear polynomial and individual voltage outputs were used. Since the voltage output of each sensor (obtained from tests) contained both velocity and yaw angle, an initial value which was slightly more than the free stream velocity was assumed and the yaw angle for each sensor was calculated. The assumed velocity and the three yaw angles were then compared with the three components of velocity which were based on the direction cosines of each sensor (with reference to the arrangement in the experimental setup). Iteration was performed until the velocity assumed equalled the velocity calculated.

```

C   Program to calculate alpha1, alpha2, alpha3
C   Suffix 1,2 and 3 stands for sensor 1,3 and 5 resply.
C   PARAMETER ndat IS THE TOTAL NUMBER OF VOLTAGES TO BE READ

parameter (ndat1=6000,slope=3.05175781e-4,offset=-10.0)
character*15 fname1,fname2,fname3
dimension C1(ndat1),C2(ndat1),C3(ndat1),UX(ndat1)
dimension UY(ndat1),UZ(ndat1)
dimension V1(ndat1),V2(ndat1),V3(ndat1)
C   implicit real*8 (a-h,o-z)
real a1(10),a2(10),a3(10),n1,n2,n3,v1,v2,v3,
+um,alpha1,alpha2,alpha3,rhs1,rhs2,rhs3,lhs1,
+lhs2,lhs3,err1,err2,err3,dc(3,3),cosalf(3),vel(3),
+error,newum

C   write(*,*) 'Give the total number of data points'
C   read(*,*) ndat

open(unit=50,file='newum.dat',type='new')
open(unit=14,file='coef1.dat',type='old')
open(unit=15,file='coef2.dat',type='old')
open(unit=16,file='coef3.dat',type='old')
open(unit=25,file='test#',type='old')
open(unit=30,file='txyz',type='new')
open(unit=35,file='tavg',type='new')

C   READ VALUES OF VOLTAGE FROM DATA FILE (WAVE TANK)

ndat=900

79  do k=1,ndat
read(25,*) C3(k),C2(k),C1(k)
V1(k)=((slope*C1(k))+offset)*1.01499572
V2(k)=((slope*C2(k))+offset)*0.916097321
V3(k)=((slope*C3(k))+offset)*1.084442167
end do

C   READ IN EXPONENTS OF THREE SENSORS
read(14,*) n1
read(15,*) n2
read(16,*) n3

C   READ IN COEFFICIENTS FOR THE THREE SENSORS

read(14,*) (a1(i), i=1,10)
read(15,*) (a2(i), i=1,10)
read(16,*) (a3(i), i=1,10)

```

```

5  continue
   if(err1.gt..01) then
   alpha1=alpha1+.01

   rhs1=a1(3)*alpha1+a1(5)*alpha1*(um**n1)+a1(6)*(alpha1**2)+
   + a1(8)*alpha1*(um**(2*n1))+a1(9)*(alpha1**2)*(um**n1)+
   + a1(10)*(alpha1**3)

   err1=(lhs1-rhs1)/lhs1
   go to 5
   endif
C  write(*,*)'alpha1 = ',alpha1,'err1 = ',err1

   if(err2.lt.0.) then
C  write(*,*) 'Starting alpha2 - TOO LARGE !'
   endif

10  continue
   if(err2.gt..01) then
   alpha2=alpha2+.01

   rhs2=a2(3)*alpha2+a2(5)*alpha2*(um**n2)+a2(6)*(alpha2**2)+
   + a2(8)*alpha2*(um**(2*n2))+a2(9)*(alpha2**2)*(um**n2)+
   + a2(10)*(alpha2**3)

   err2=(lhs2-rhs2)/lhs2
   go to 10
   endif
C  write(*,*)'alpha2 = ',alpha2,'err2 = ',err2

   if(err3.lt.0.) then
C  write(*,*) 'Starting alpha3 - TOO LARGE !'
   endif

15  continue
   if(err3.gt..01) then
   alpha3=alpha3+.01

   rhs3=a3(3)*alpha3+a3(5)*alpha3*(um**n3)+a3(6)*(alpha3**2)+
   + a3(8)*alpha3*(um**(2*n3))+a3(9)*(alpha3**2)*(um**n3)+
   + a3(10)*(alpha3**3)

   err3=(lhs3-rhs3)/lhs3
   go to 15
   endif
C  writ(*,*)'alpha3 = ',alpha3,'err3 = ',err3

```

```

m=3
dc(1,1)=0.7071
dc(1,2)=0.
dc(1,3)=0.7071
dc(2,1)=0.7071
dc(2,2)=0.6124
dc(2,3)=-0.3536
dc(3,1)=0.7071
dc(3,2)=-0.6124
dc(3,3)=-0.3536

```

```

cosalf(1)=cos(alpha1)*um
cosalf(2)=cos(alpha2)*um
cosalf(3)=cos(alpha3)*um

```

C 'ELIM' AND 'SUBST' ARE SUBROUTINES TO SOLVE THREE LINEAR EQUATIONS

```

call elim(m,dc,cosalf)
call subst(m,dc,cosalf,vel)

```

```

C write(*,*)'vel vals for data set ',icount
do 30 i = 1,3
C write(*,*)vel(i)
30 continue
newum=sqrt(vel(1)**2 + vel(2)**2 + vel(3)**2)
error=(newum-um)/newum
if(error.lt.0.01) then
um=um-0.01
go to 20
endif
C write(*,*)newum='newum',error='error',for data set ',icount
write(50,*) newum
C write(30,*)'The following are the values of UX, UY, UZ'
write(30,*) vel(1),vel(2),vel(3)
sumx = vel(1) + sumx
sumy = vel(2) + sumy
sumz = vel(3) + sumz
icount = icount + 1
if (icount.gt.ndat) go to 500
go to 99
500 asumx = sumx/ndat
asumy = sumy/ndat
asumz = sumz/ndat
C write(35,*)'Average of UX, UY, UZ'
write(35,*) asumx,asumy,asumz
stop
end

```

```

subroutine elim(n,a,c)
  real a(3,3),c(3)
  integer l,n,x
  l=n-1
  do 30 l=1,l
    ix=il+1

    call pivot(n,a,c,ix,il)
    do 20 i2=ix,n
      do 10 j=ix,n
        a(i2,j)=a(i2,j)-a(i2,il)/a(il,il)*a(il,j)
10      continue
        c(i2)=c(i2)-a(i2,il)/a(il,il)*c(il)
20      continue
30      continue
    return
  end

subroutine subst(n,a,c,f)
  real a(3,3),c(3),f(3),sum
  integer l,n,ix,jx
  l=n-1
  f(n)=c(n)/a(n,n)
  do 10 ix=1,l
    sum=0
    i=n-ix
    j=i+1
    do 20 jx=j,n
      sum=sum+a(i,jx)*f(jx)
20    continue
    f(i)=(c(i)-sum)/a(i,i)
10  continue
  return
  end

subroutine pivot(n,a,c,ix,il)
  real a(3,3),c(3),big,temp,dum,am
  integer j,n
  jj=il
  big=abs(a(il,il))
  do 10 i=ix,n
    am=abs(a(i,il))
    if(am.gt.big) then
      big=am
      jj=i
    endif
10  continue

```

```
if(jj.ne.i1) then
do 20 j=i1,n
dum=a(j,j)
a(j,j)=a(i1,j)
a(i1,j)=dum
```

```
20 continue
```

```
temp=c(jj)
c(jj)=c(i1)
c(i1)=temp
endif
return
end
```



